Russian Chemical Reviews **83** (8) 758 – 782 (2014) © 2014 Russian Academy of Sciences and Turpion Ltd

DOI 10.1070/RC2014v083n08ABEH004402

Chemical vapour-phase deposition of ruthenium-containing thin films

V Yu Vasilyev,[a, b] N B Morozova,[c] I K Igumenov [c]

[a] *Novosibirsk State Technical University*
Prosp. K Marksa 20, 630073 Novosibirsk, Russian Federation
[b] *'SibIS', Limited Liability Company*
Krasnyi prosp. 220/2, 630049 Novosibirsk, Russian Federation
[c] *A V Nikolaev Institute of Inorganic Chemistry, Siberian Branch of the Russian Academy of Sciences*
Prosp. Academika Lavrentieva 3, 630090 Novosibirsk, Russian Federation

Chemical and materials science aspects of formation of ruthenium-containing thin films for modern high-precision technologies by chemical vapour deposition (CVD) methods are considered. Chemical approaches to the synthesis of main precursors used in MOCVD techniques, layer growth processes as well as main physicochemical and electrical properties of ruthenium-containing thin films are analyzed.
The bibliography includes 120 references.

Contents

I. Introduction 758
II. Main problems in deposition of ruthenium-containing coatings 760
III. Main ruthenium precursors and their characteristics 761
IV. Ruthenium films 769
V. Ruthenium dioxide films 778
VI. Examples of other ruthenium-containing materials 778
VII. Conclusion 779

I. Introduction

Progress in the development of modern high-precision devices is governed by the design of novel materials and emergence of new technologies. The greatest progress is characteristic of microelectronics that utilizes the advances achieved in technology and materials science. Since the end of the 20th century, the development of microelectronics in the short, mid and long term has follows the International Technology Roadmap for Semiconductors (ITRS).† The roadmap covers all aspects of the development of microelectronics including the design of microelectronic devices, technology (photolithography, metallization, control), integration of technological processes, production of microelectronic devices, *etc*. The requirements for technology and advanced materials are revised biennually based on analysis of a vast variety of information sources by analytical groups from the USA, European Union, Japan, South Korea and Taiwan. In essence, the roadmap specifies directions of activity for all research institutions, design organizations, production facilities, equipment and material manufacturers involved in practice in the field of microelectronics.

The search for and applicability assessment of novel materials belong to key avenues of progress in microelectronics. For instance, starting with the 2005 ITRS, the 'Interconnect' Section concerning technology and materials for microelectronic devices has included an analysis of prospects for application of metallic ruthenium and ruthenium oxide thin films. This gave an impetus to corresponding investigations. Most published studies on ruthenium-containing thin films and coatings fabricated from ruthe-

V Yu Vasilyev Doctor of Chemical Science, Professor at the NSTU, Deputy Director General of the SibIS LLC. Telephone (7-383) 227 76 39, e-mail: vasiliev@sib-is.ru
Current research interests: thin films, CVD processes, technology of micro- and nanoelectronic devices.
N B Morozova Doctor of Chemical Science, Leading researcher of the NIIC SB RAS. Telephone (7-383) 330 95 56, e-mail: mor@niic.nsc.ru
Current research interests: chemistry of volatile metal complexes with organic ligands, CVD processes.
I K Igumenov Doctor of Chemical Science, Professor, Head of the Laboratory for Chemistry of Volatile Coordination and Organometallic of the NIIC SB RAS. Telephone (7-383) 333 05 54, e-mail: igumen@niic.nsc.ru
Current research interests: chemistry of volatile coordination and organometallic compounds, coating formation by CVD methods.

Received 24 April 2013
Uspekhi Khimii **83** (8) 758 – 782 (2014); translated by A M Raevskiy

† The ITRS materials are public domain and available only from the Website http://www.itrs.net.

nium, ruthenium oxides or other ruthenium-containing compounds were aimed at utilizing these materials in high-precision (first of all, microelectronics) technologies.

The practical orientation of studies on the growth of ruthenium-containing films predetermined the character of publications on the subject. They mainly include a brief description of experiments and results of characterization of the composition, structure and properties of coatings prepared by one or another method; in some cases, the applicability of coatings to solve particular problems in microelectronics is analyzed. Since the publication of pioneering studies,[1–3] ruthenium coatings have been studied in most detail, while coatings prepared from ruthenia, RuO_2, have been less studied.

Pioneers in the research on ruthenium-containing coatings treated them as candidate materials for electrodes,[1] contacts,[2] VLSI metallization,[3] as electrode materials in Metal–Insulator–Metal (MIM) capacitor memory cells,[4] as materials for transistor gates,[5] barrier films,[6] seed layers for 'copper' multilayer metallization of integrated circuits (IC),[7] and for various applications in nanotechnology.[8–11] Taking the schematic of a capacitor memory cell shown in Fig. 1 *a* as an example, one can see that utilization of ruthenium as electrode material requires taking account of different-nature materials, *viz*., TiN (contact), silica support, insulator (Ta_2O_5, Al_2O_3, HfO_2) and other materials and their combinations if necessary.

Most publications concerning the deposition of ruthenium films were reported by researchers from South Korea and Japan. This is due to intensive research on fabrication of integrated circuits for dynamic memory devices with MIM capacitor memory cells carried out in these countries.

The interest in RuO_2 is due to its low specific resistance that is only slightly different from that of ruthenium (~ 35 *vs.* ~ 7 $\mu\Omega$ cm, respectively).[1–3] This enables the appearance of conductive films on ruthenium surface; the surfaces of aluminium- and copper-based materials traditionally used in microelectronics can be coated with insulating oxides that induce an inadmissible increase in the resistance of conductors. The problem of formation of conductive films becomes topical in connection with miniaturization of microelectronic devices and, as a consequence, with the need for continuous decrease in the thickness of thin film materials in the future-generation devices. For metallic ruthenium whose surface film can bear RuO_2 impurity, the problem is much less significant.

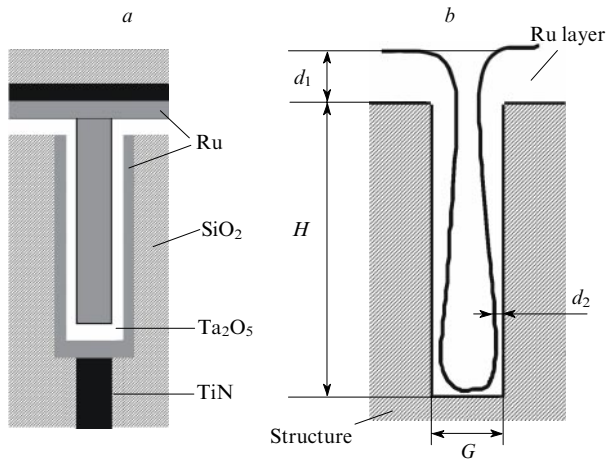


Figure 1. Cross sections: a simplified MIM memory cell with thin ruthenium films as capacitor electrodes (*a*) and a 3D rectangular structure (*b*).[4]

Methods of preparation of ruthenium-containing coatings vary with time. Sputtering of ruthenium from appropriate targets [physical vapour deposition (PVD) technique] used from ~ 1978 [12] to ~ 2000 (authors of the most recent publications [13–15] treated sputtering as basic comparative method) is followed by chemical vapour-phase deposition (CVD) and metal-organic CVD (MOCVD) utilized since 1985 up to date. Pulsed MOCVD (PMOCVD) methods have been developed since 2003. Going to novel processes was dictated by toughening of requirements for conformality (thickness ratio d_2/d_1, see Fig. 1 *b*) of coatings on semiconductor structures with complicated relief, which is usually characterized by the aspect ratio

$$\mathrm{AR} = \frac{H}{G}$$

The PVD technique is of limited use in fabrication of complex 3D microelectronic devices owing to non-conformal coating of lateral steps with materials being deposited. Also, narrow gaps between functional units of the device remain unfilled at low conformality and undesired voids are formed.[16] The requirement for conformality of coatings of the structures with high aspect ratios is of particular importance for modern microelectronics technology. Chemical vapour-phase deposition methods are more promising for application to complex 3D systems. Most authors treat the MOCVD process as pyrolysis of vapours of organometallic compounds. A CVD process can occur in the presence of a reactive second reactant and, in particular, involve the formation of intermediates of the reaction between reactants in the vapour phase. In this review, such processes are denoted as MOCVD, which means a CVD process using any volatile metal complexes with organic ligands (precursors) irrespective of their structures. A distinctive feature of CVD techniques is efficient control of parameters of the process and, therefore, the properties of films and nanostructures (nanocrystallite size, coating thickness, structure and morphology); these methods make it possible to prepare highly conformal coatings on complex-shape systems.[17, 18]

Recently, in connection with complication of the shape of microelectronic devices and the need for preparation of thin conformal coatings, a MOCVD technique with pulsed consecutive feed of reactants and purge gas (so-called PMOCVD method) has been developing intensively. Here, deposition occurs in cyclic manner; the overall deposition cycle using two initial reactants involves four consecutive pulses of precursor vapours, purge gas, second reactant and purge gas again. In some cases, more complicated designs are used, which involve intermediate evacuation of the reaction chamber.

A number of reaction systems allow films to grow in the so-called atomic layer deposition (ALD) regime provided optimized temperature conditions, cyclic regime, appropriately chosen reactant doses and particular temperature ranges.[19] Usually, ALD processes can be practically implemented using precursors that are prone to chemical inter-

action with the substrate (chemisorption). The limiting stage of the overall ALD process that is entirely localized on the surface of a sample is the interaction of the chemisorbed precursor with the second reactant deposited on the surface from the vapour phase provided that all adsorption sites are filled to achieve self-limiting growth of the film. With this mechanism, film deposition in the ALD regime should provide layer-by-layer growth and, as a consequence, almost 100% degree of conformality of the deposited films on the inner surfaces of complex-shape 3D structures. However, no optimal reactants and layer growth conditions in the ALD regime have been reported to date since publication of the pioneering study[20] on ALD of ruthenium.

An analysis of published data showed that main difficulties in the preparation of ruthenium films are due to sensitivity of ruthenium precursors to the substrate material (properties) and to poor nucleation of ruthenium in the initial steps of film growth and, consequently, slower deposition rate (so-called nucleation delay, Fig. 2). This leads to formation of various polycrystalline films, namely, thin films are of island type while thick films are characterized by certain grain size distribution and high surface roughness; this negatively influences the density and resistance of the films and, therefore, makes them of limited use in microelectronics.

Better ruthenium nucleation with shorter or even zero nucleation delays can be attained by plasma activation of the second reactants [so-called plasma-activated CVD (PACVD)].[21,22] This technique allows one to improve nucleation on flat surfaces of various materials, but fast recombination of radicals in the vapour phase precludes the preparation of conformal coatings on complex-shape 3D structures.[17]

In this connection, there has been increasing interest in search for thermally activated MOCVD processes of the synthesis of ruthenium films with minimal nucleation delays. Such a search is carried out in two directions. One way is to shorten the nucleation delay by pre-treatment of the surface by plasma discharge,[23] UV radiation, ozone[24] or titanium tetrachloride vapours.[25] The other one involves the use of novel precursors characterized by enhanced adsorption capacity which may lead to shortening of the nucleation delay.

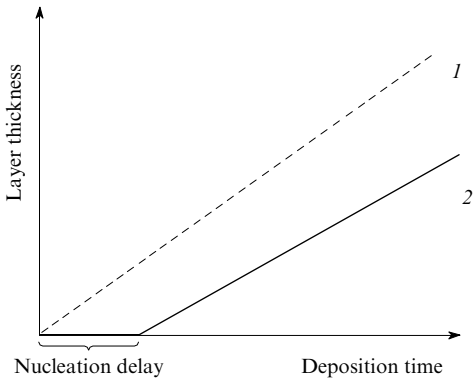


Figure 2. Film thickness-*vs*.-time plots for CVD of ruthenium: conventional CVD at a constant rate (*1*) and CVD with nucleation delay in the initial step of the growth process (*2*).

Most recent studies were focused on characterization of deposited films and present only a brief description of experiments. We believe such publications are little informative because a correct examination and comparison of the reasons underlying long nucleation delays are impossible. Owing to a huge amount of information on various methods for vapour phase deposition of ruthenium-containing coatings available in the literature, in this review we will analyze the results of the most representative publications reported in the last fifteen years. The emphasis is placed on the publications concerning metallic ruthenium films; data on ruthenium oxide films and films prepared from other compounds are only briefly analyzed.

II. Main problems in deposition of ruthenium-containing coatings

A key advantage of thin-film materials prepared by MOCVD methods consists in that their synthesis is part of the technological process of fabrication of, *e.g.*, integrated circuits. Therefore, the quality and reproducibility of the properties of thin films to a great extent predetermine the performance and parameters of microelectronic devices and the nominal product yield.

Main problems in the deposition of thin films including ruthenium-containing coatings by MOCVD methods on the surface of microelectronic devices fabricated on either pilot or full scale (here, the main item is usually a semiconductor wafer 100–300 mm in diameter and less than 1 mm thick) are as follows:[18,26]

— search for precursors or their combinations to prepare thin films (taking into account simplicity, convenience and reproducibility of the process);

— search for reactor (more generally, equipment) designs to attain high performance, maximum uniformity (uniform thickness) of the deposited material and industrial safety;

— macrodefectness reduction of thin films (minimization of the amount of microparticles on the surface or within the deposited film);

— low conformality of film growth within 3D fragments of integrated circuits;

— quality control and optimization of deposition process to attain the highest degree of utilization of the precursor and reproducibility of parameters of the thin films.

Practical implementation of MOCVD methods requires establishment of some correlations between the growth rate (can be obtained in studies of deposition kinetics), coating composition, physicochemical and electrical (electrophysical) properties of the coating and the 'input' parameters of the deposition process.[18] The 'input' parameters usually include a number of key process parameters, such as the wafer temperature, the temperature of the precursor vapour source, volume rate of reagent gas, pressure in the reaction chamber, *etc*. Also, as applied to microelectronics technologies, one should monitor deviations of all target values from their average values within the sample (a semiconductor wafer to 300 mm in diameter and to 450 mm in diameter in the near future).

III. Main ruthenium precursors and their characteristics

1. Precursors for MOCVD deposition of ruthenium-containing films

Researchers are focused on the search for precursors, their combinations with other reactants (mainly oxygen) and optimal MOCVD regimes to provide the necessary composition, structure and properties of ruthenium-containing coatings on various materials for, *e.g.*, MIM memory cells.

Physicochemical properties of compounds used in MOCVD processes play an important role because they specify the parameters of experiments, the design of key units of CVD equipment and, eventually, the properties of the deposited films. Practical implementation of MOCVD processes requires precursors that should have the following properties:

— a precursor should sublime without decomposition, *i.e.*, be thermally stable in the condensed phase at the evaporation temperature for a period necessary to carry out the deposition process;

— the saturated vapour pressure of a precursor should be rather high (highly volatile compound) to provide a necessary concentration of vapours in the reaction zone;

— a precursor should be stable in the vapour phase and the decomposition temperature of its vapours on the heated surface should exceed the evaporation temperature; if the evaporation and decomposition temperatures are close, thermal decomposition of the precursor vapours will occur on the surface of the heated feed lines and(or) in the bulk of the reactor rather than on the substrate surface (this will lead to great loss of the precursor, reduction of the efficiency of the deposition process and to changes in the coating structure owing to codeposition of large clusters that are formed in the vapour-phase reactions;

— a precursor should undergo complete decomposition to volatile products, except the coating material (nonvolatile decomposition products will co-deposit with the coating material on the substrate);

— it is desirable to conduct deposition processes at moderate temperatures because in this case the design of the unit is simplified and the range of the substrate materials extends; carrying out deposition of coatings at high temperatures sometimes induces secondary decomposition reactions of organic products that lead to carbonization of the films;

— precursor vapours and products of its thermal decomposition should be inert towards the substrate and unit materials;

— for convenience of operation, it is important that the precursor be low toxic or nontoxic, as well as stable in air and on storage;

— economically, it is required that the target compound be synthesized in high yield and the initial reactants be commercially available.

Thus, a correct choice of the initial compounds requires information on first of all their volatility, thermal stability, stability in air, toxicity, synthetic availability/accessibility and some other parameters.

In the case of MOCVD methods, the range of ruthenium precursors is limited to a few classes of volatile organometallic and coordination compounds that can be divided into four groups depending on the nature of ligands and their derivatives. Three groups include carbonyls, cyclopentadienyls, and β-diketonates. The fourth group includes some other precursors that were studied by a number of research groups. The following ruthenium compounds were reported as precursors in the literature:

hetero-ligand metal carbonyls: $Ru(hfac)_2(CO)_2$ (hfac is hexafluoroacetylacetonate), $Ru_3(CO)_{12}$, $RuL_y(CO)_z$ (L is β-diketonate), $[Ru(Cp)(CO)_2]_2$ (Cp is η^5-cyclopentadienyl), $Ru(acac)(CO)_2$, (acac is acetylacetonate), $Ru(diene)(CO)_n$, $RuL(CO)_4$, $Ru(chd)(CO)_3$ (chd is η^4-cyclohexa-1,3-diene), $[RuL_2(CO)_2]$;

cyclopentadienyl derivatives: $Ru(Cp)_2$, $Ru(Cp')_2$ (Cp′ is methyl-η^5-cyclopentadienyl), $Ru(EtCp)_2$ (EtCp is ethyl-η^5-cyclopentadienyl), $Ru(Cp^*)_2$ (Cp* is pentamethyl-η^5-cyclopentadienyl), $Ru(dmpd)_2$ (dmpd is 2,4-dimethylpentadienyl), Ru(dmpd)(Cp), Ru(dmpd)(Cp′), Ru(dmpd)(EtCp), $Ru(Pr^iCp)_2$ (Pr^iCp is isopropyl-η^5-cyclopentadienyl), $Ru(Cp)(Pr^iCp)$, $Ru(dmpd)(Pr^iCp)$, Ru(Cp′)(EtCp), $Ru(od)_3$ (od is octa-2,4-dionate);

β-diketonates: $Ru(acac)_3$, $Ru(thd)_3$ (thd is 2,2,6,6-tetramethylhepta-3,5-dionate), $Ru(thd)_2(cod)$ (cod is cycloocta-1,5-diene), Ru(cod)(PhMe) (PhMe is toluene), Ru(chd)(PhH) (PhH is benzene), IMBCHRu [(1-isopropyl-4-methyl-η^6-benzene)(η^4-cyclohexa-1,3-diene)ruthenium];

other precursors including allyl derivatives $Ru(All)_2(cod)$ (All is η^3-allyl), Ru(All)(Cp)(CO), $Ru(MeAll)_2(cod)$ (MeAll is methyl-η^3-allyl); nitrogen-containing compounds, *e.g.*, $Ru(Bu^t\text{-Me-amd})_2(CO)_2$ (Bu^t-Me-amd is *N*,*N*′-di-*tert*-butylacetamidinate), dithiocarbamates $Ru(Et_2NCS_2)_2(CO)$, $Ru(S_2PPh_2)_2(PPh_3)_2$, $Ru(S_2PPh_2)_2(PPh_3)(CO)$ and some other compounds.[27–78]

Note that the first three classes of base precursors were mentioned in the pioneering publication [3] on the deposition of ruthenium and RuO_2. That study was the first one devoted to investigation of the possibility of MOCVD deposition of ruthenium and RuO_2 in a low-pressure tube reactor with hot walls using three different ruthenium-containing precursors, *viz.*, $Ru_3(CO)_{12}$, $Ru(Cp)_2$ and $Ru(acac)_3$. Figure 3 presents the chronology of and main trends in the development of chemistry of ruthenium-containing precursors. A general trend is that the chemical composition of precursors that were for the first time described in Ref. 3 becomes more complicated.

A necessary condition for sublimation of a solid precursor at moderate temperatures is that the energy of intermolecular bonds (van der Waals forces, electrostatic and dipole interactions) in the structure be much lower than the energy of intramolecular bonds. Therefore, the volatility and thermal stability of a compound are first of all related to its structural parameters and electronic structure. In the last decade, methods for deposition of ruthenium were developed in order to search for 'ideal' precursor suitable for formation of conformal ruthenium thin films with low specific resistance on particular surfaces of 3D systems with high aspect ratios. Note that search for novel reactants is also due to the need to find a non-infringing precursor for industrial applications (ideally, a liquid with high vapour pressure).

Usually, particular deposition processes are developed using empirical choice of initial compounds because of limited fundamental knowledge and the lack of generalizations concerning physical chemistry of precursors; therefore, an analysis of the totality of their thermal parameters is an important step in the development of MOCVD processes.

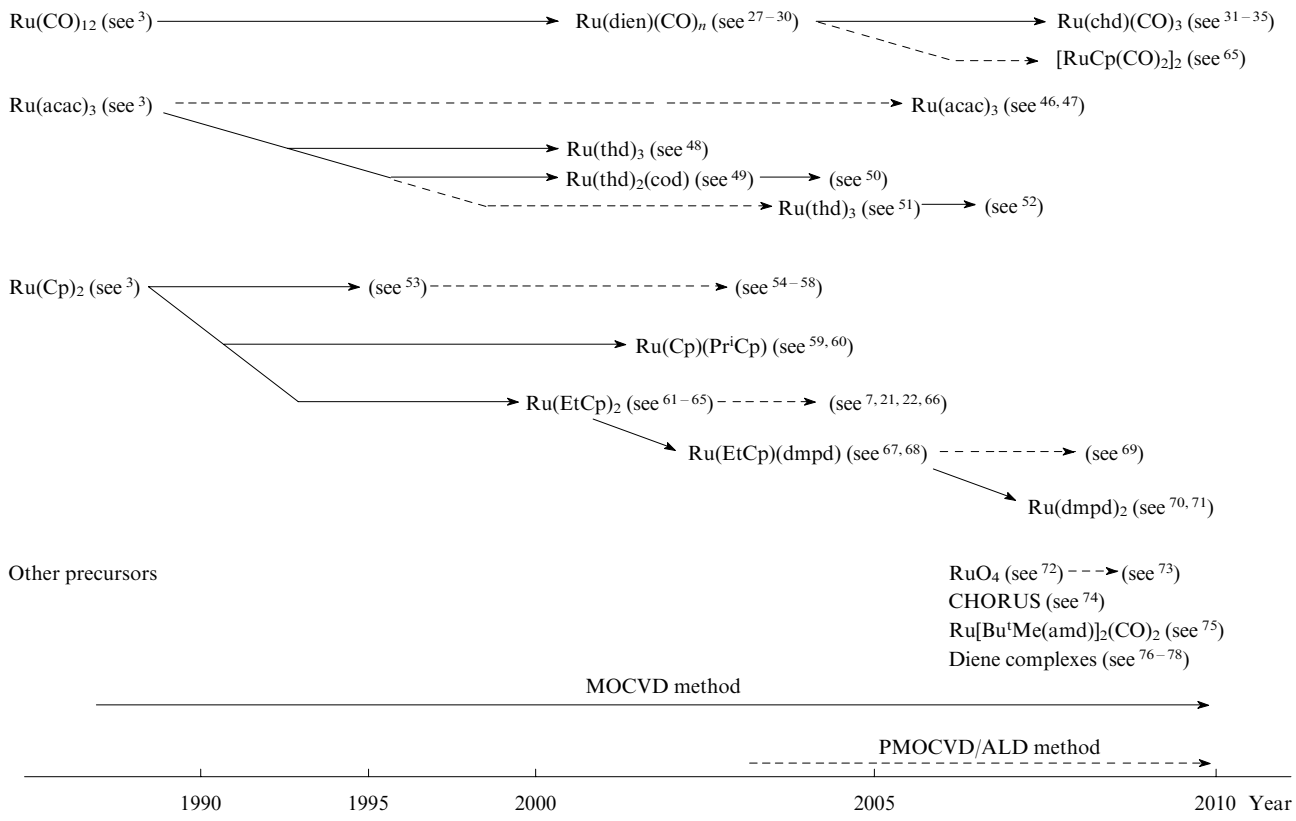


Figure 3. Chronology of studies on precursors used to prepare ruthenium thin films.

2. Methods of investigation of thermal properties of precursors

During the deposition of films and coatings, precursors usually spend a long time in the condensed phase at high temperatures. Modern technologies require that the precursor be highly stable at the sublimation (evaporation) temperature. In this case, often the limiting parameter that predetermines the possibility of using a crystalline compound in MOCVD processes is its thermal stability, *i.e.*, stability in the solid phase on heating to a specified temperature without changing the chemical composition. Usually, thermal stability is characterized by the temperature at which changes in the chemical composition begin. This temperature is determined by thermal analysis methods. Thermal stability of compounds in the condensed state is most often determined by differential thermal analysis (DTA), thermogravimetric analysis (TGA) and differential scanning calorimetry (DSC). Theoretical foundations of these methods and relevant methodological approaches are available in a monograph.[79] A feature of these methods is the possibility of determining such an important parameter, as the initial temperature of the reaction between precursors with reagent gases (*e.g.*, hydrogen or oxygen). By comparing the results of the studies of different compounds in identical conditions (at equal heating rates and sample weight, possibility of gas diffusion towards the sample, *etc.*) one can compare the behaviour of precursors on heating.

Yet another important characteristic of MOCVD precursors is volatility, *i.e.*, the ability to sublime without deposition. Currently, the main source of information on the volatility and thermodynamic parameters of vaporization are experimental measurements of the saturated vapour pressure ($P-T$ plots) whose results are represented in the form

$$\ln P = B - \frac{A}{T}$$

where the coefficients A and B are related to the thermodynamic parameters of vaporization (changes in enthalpy ΔH and entropy ΔS) as follows:

$$A = \frac{\Delta H_{T^*}}{R},$$

$$B = \frac{\Delta S_{T^*}}{R}$$

(T^* is the midpoint of the temperature range in which the vapour pressure was measured).

Experimental data on the vapour pressure of a precursor make it possible to estimate the concentration of vapours in the vapour phase at a particular temperature and, therefore, to control the evaporator temperature in MOCVD processes.

Various methods of determination of saturated vapour pressure are available, *viz.*, static, quasi-static, dynamic (the flow and Langmuir methods) and kinetic ones (various modifications of Knudsen effusion procedure).[80, 81]

Yet another important characteristics of precursors is thermal stability of vapours on a heated surface. This characteristics may play a decisive role in choosing some experimental parameters of the process, such as the deposition temperature and the need for introducing reactive additives (hydrogen, oxygen, *etc.*). *In situ* high-temperature mass spectrometry studies on thermal decomposition of vapours in the 'isolated molecule' approximation began in Refs 82–84. The term 'thermal stability of vapours' means the initial temperature at which heterophase transformations of precursor vapours to products of thermal decomposition on a heated surface begin. Unlike the condensed phase, here one deals with studies on the decomposition of individual molecules adsorbed on the surface.

Mechanisms of thermal decomposition of vapours are studied using a thermal reactor attached to a mass spectrometer.[82] A molecular beam from the reactor passes through an effusion orifice into the ionization chamber of the mass spectrometer used to determine the composition of the vapour phase. Also, the reaction gas can be supplied to the inlet of the reactor. This makes it possible to study how the reaction gas influences the decomposition of the precursor vapour. The gas flow in all compartments of the system is molecular in character. This excludes the possibility of reactions of the starting compounds with decomposition products and the effect of diffusion on the reaction kinetics. The procedure allows one to carry out experiments in a wide temperature range and to detect both primary reaction products and deep stages of decomposition of compounds by monitoring qualitative changes in the composition of volatile products of thermolysis. Information on the process has the form of temperature dependences of the intensities of ion currents in the mass spectrum under stepwise increase in the temperature in the reactor. Based on analysis of these plots, one can suggest the most possible pathways of thermal decomposition of the precursor vapours. Now we will consider main classes of ruthenium precursors.

3. Ruthenium carbonyls and their derivatives

Trinuclear carbonyl $Ru_3(CO)_{12}$ is one of the most readily available ruthenium precursors. This is a red-orange powder with a melting point of about 150 °C. The molecular structure and packing of $Ru_3(CO)_{10}$ in the crystal according to X-ray diffraction data[85] are shown in Fig. 4. Metal carbonyls are synthesized by reactions of carbon monoxide with metals or metal salts at elevated temperatures and pressures. The carbonyl $Ru_3(CO)_{12}$ can also be obtained by illuminating or heating ruthenium pentacarbonyl[86]

$$3\,Ru(CO)_5 \longrightarrow Ru_3(CO)_{12} + 3\,CO \qquad (1)$$

In turn, ruthenium pentacarbonyl $Ru(CO)_5$ is synthesized[86] from ruthenium iodide in the presence of copper or silver

$$RuI_3 + 3\,Cu + 8\,CO \longrightarrow Ru(CO)_5 + 3\,Cu(CO)I \qquad (2)$$

Melting of the compound with decomposition can be due to interactions between carbon atoms C(21)···C(11)···C(31) and C(22)···C(12)···C(32) (see Fig. 4 *a*) that result in the formation of a sterically hindered conformation of the molecule.[85]

Information on the thermal properties of $Ru_3(CO)_{12}$ is limited to the data of measurements of the $P-T$ plot (Fig. 5). They were used to calculate the thermodynamic parameters of sublimation.[87] The precursor has a drawback, namely, a narrow stability interval (up to 150 °C).

Hetero-ligand carbonyls bearing diene, β-diketonate and other ligands are synthesized by reactions of $Ru_3(CO)_{12}$ with ligand sources in toluene or other organic solvents on heating in inert atmosphere.[30] The yields of these reactions can be as high as 90%. The reaction of $Ru_3(CO)_{12}$ with cyclohexa-1,3-diene carried out in dry argon atmosphere in the presence of toluene over a period of 24 h results in a hetero-ligand complex $Ru(CO)_3(chd)$[32] representing a bright-yellow opalescent liquid with a vapour pressure ranging from 0.28 to 5 Torr in the temperature range 5–80 °C (estimate). The complex can also be synthesized by thermolysis of $Ru_3(CO)_{12}$ in cyclohexane for 24 h and isolated chromatographically from the dichloromethane–hexane system.[88] Presently, this is one of the most often used precursors with such attractive properties, as the aggregation state (liquid) and high vapour pressure.

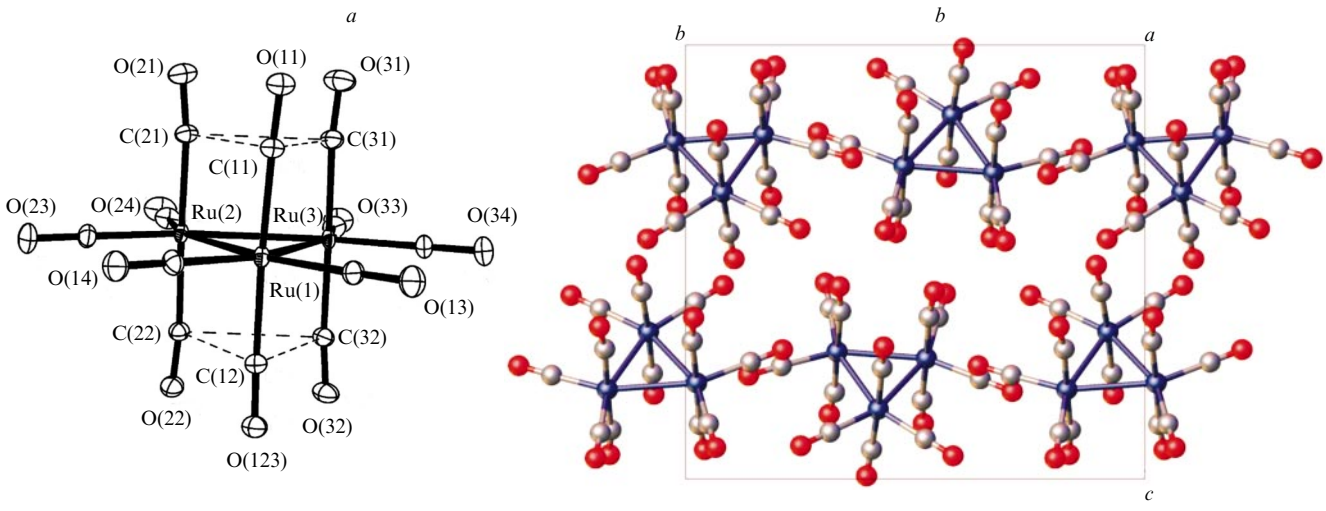


Figure 4. Molecular structure (*a*) and packing of $Ru_3(CO)_{10}$ in the crystal (*b*).[85]

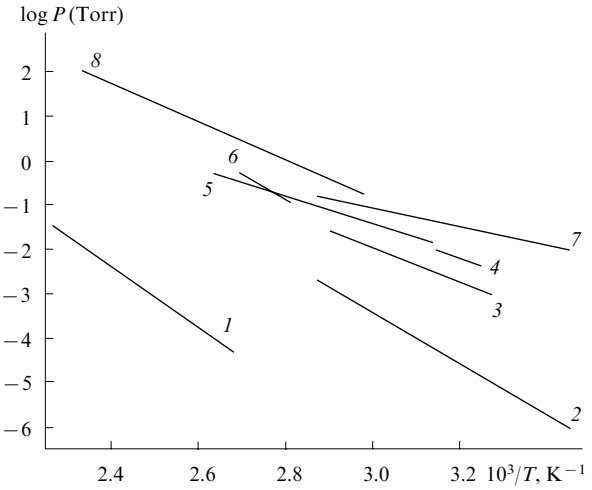


Figure 5. $P-T$ plots for ruthenium complexes.[87] $Ru(acac)_3$ (*1*), $Ru_3(CO)_{12}$ (*2*), $Ru(All)_2(cod)$ (*3*), $Ru(All)_2(nbd)$ (*4*), $Ru(EtCp)_2$ (*5*), $Ru(Cp)_2$ (*6*), $Ru(Pr^iCp)_2$ (*7*) and $Ru(hfac)_3$ (*8*). Compounds $Ru(acac)_3$, $Ru_3(CO)_{12}$, $Ru(EtCp)_2$ and $Ru(hfac)_3$ are commercially available products.

4. Ruthenium β-diketonates

Among ruthenium precursors, ruthenium(III) β-diketonates have been best studied. These compounds are usually synthesized by reactions of β-diketonate ligands with metal ions in aqueous-ethanol solutions: $Ru(acac)_3$,[89–91] $Ru(tfac)_3$,[91–93] and $Ru(bac)_3$[90,92] (tfac is trifluoroacetylacetonate and bac is 1-phenylpentane-2,4-dionate). Compound $Ru(acac)_3$ was for the first time synthesized in the early 20th century by reaction of $RuCl_3$ and acetylacetone in the presence of potassium bicarbonate on heating (15% yield).[89] Subsequently the synthetic procedure was only slightly changed. The major drawback of this approach consists in a low yield of final products owing to competition of anionic ligands and β-diketones for coordination sites. This leads to formation of polymeric forms in solution, where β-diketonate fragments (can also act as bridging ligands) co-exist with coordinated ions, Cl^- and OH^-.

To synthesize other compounds from this class with the general formula RuL_3 [L = acac, tfac, hfac, thd, ptac (ptac is 5,5-dimethyl-1,1,1-trifluorohexane-2,4-dionate), bac, btfac (btfac is 1-phenyl-4,4,4-trifluorobutane-1,3-dionate), dbm (dbm is 1,3-diphenylpropane-1,3-dionate)], a method was elaborated[87] which uses hexafluoro complexes of ruthenium and is based on replacement of fluoride ion in the inner coordination sphere. Practical implementation of the method took into account some known facts, namely, a labile behaviour of fluoride ion at low oxidation states of the metal and its low competitive ability compared to aqua ions. This method of synthesis made it possible to increase the yields of most final products to 90% and to synthesize new compounds.

Ruthenium(III) β-diketonates represent bright-red crystals, except liquid $Ru(ptac)_3$. They are insoluble in water, poorly soluble in ethanol, well-soluble in benzene, chloroform and dioxane, as well as stable on storage and nontoxic. According to X-ray diffraction data, $Ru(acac)_3$[89] and *cis*-$Ru(tfac)_3$ (Ref. 94) crystals are built of neutral molecules (this predetermines their volatility) and crystallize in the $P2_1$ space group (monoclinic crystal system); the molecules have

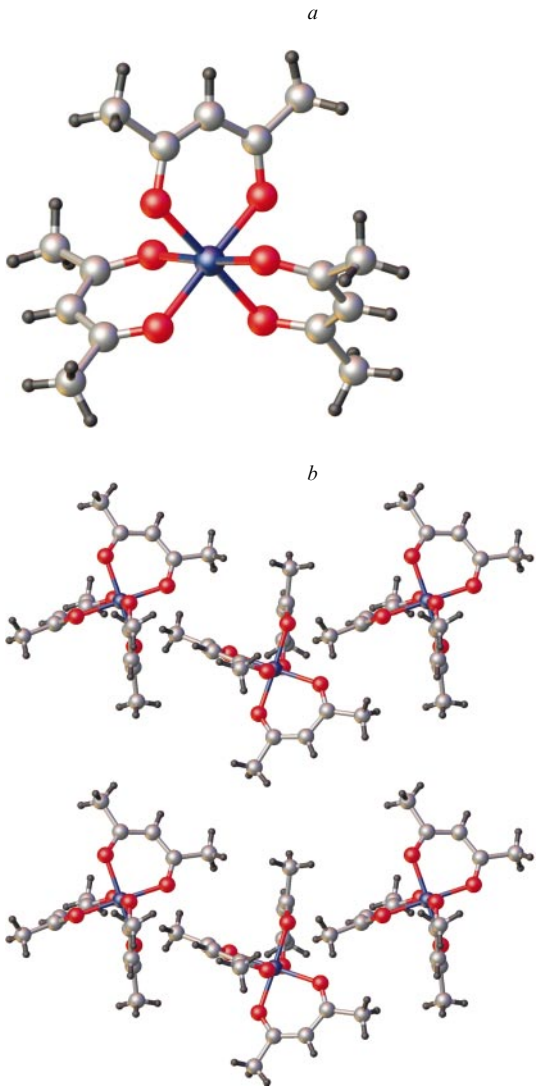


Figure 6. Molecular structure (*a*) and packing of complex $Ru(acac)_3$ (*a*) in the crystal (*b*).[89]

an octahedral coordination to six oxygen atoms from three β-diketonate ligands (Fig. 6).

Thermal properties of ruthenium(III) β-diketonates in the solid and vapour phase have been investigated in a number of studies. It was reported[95] that $Ru(acac)_3$ heated in nitrogen atmosphere undergoes partial decomposition, *viz.*, the TGA curve exhibits four steps; decomposition begins at 100 °C and the mass loss is 60% (Fig. 7 *a*). Complex $Ru(thd)_3$ heated in $N_2 + 5\%$ H_2 atmosphere sublimes without decomposition; the TGA curve demonstrates a 100% mass loss (Fig. 7 *b*). The results obtained[87] for $Ru(acac)_3$ in He stream differ from those reported in Ref. 95, namely, the process proceeds in one step and the mass loss is 20%. These differences were explained by different purities of the complexes and differences in experimental conditions.

Complexes with ligands bearing fluorinated and *tert*-butyl substituents show the highest volatility when heated in inert, oxidative and reductive atmospheres;[87] these compounds sublime without decomposition in the temperature

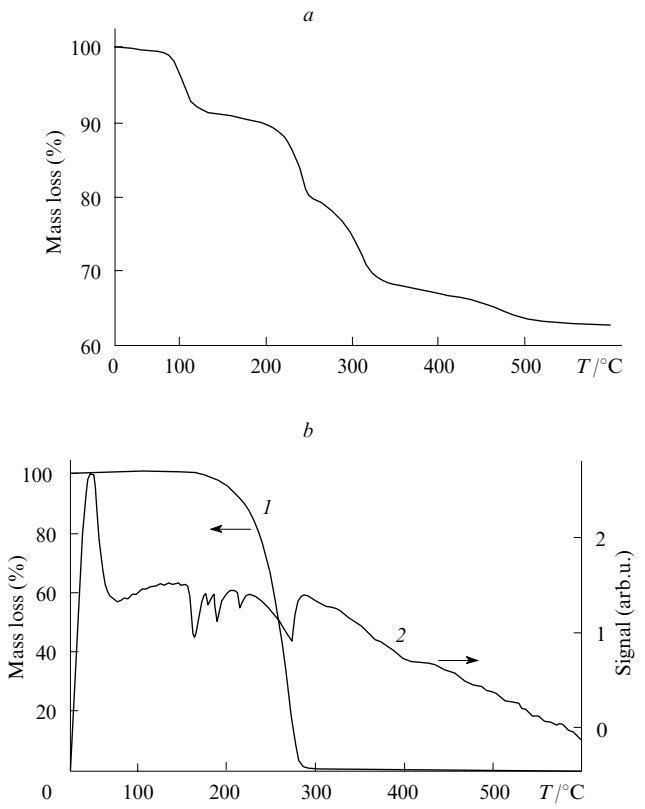


Figure 7. TGA curve obtained on heating of $Ru(acac)_3$ in N_2 atmosphere (*a*); TGA (*1*) and DTA (*2*) curves of $Ru(thd)_3$ heated in $N_2 + 5\%$ H_2 atmosphere (*b*).[95]

range from 100 to 300 °C. The order of ruthenium(III) β-diketonates with respect to volatility is as follows:

$$Ru(hfac)_3 > Ru(tfac)_3 > Ru(ptac)_3 > Ru(thd)_3 > Ru(acac)_3$$

Thermodynamic characteristics of vaporization of ruthenium(III) β-diketonates are available in the literature.[84, 96–98] The most representative series of volatility of ruthenium(III) β-diketonates has been reported.[98] The $P-T$ plots for these compounds are shown in Fig. 8. An analysis of the $P-T$ plots showed that $Ru(hfac)_3$ is characterized by the highest volatility among ruthenium(III) β-diketonates in the studied temperature ranges. On going from $Ru(acac)_3$ to $Ru(hfac)_3$ the vapour pressure considerably increases. Replacement of methyl groups by *tert*-butyl ones in the β-diketonate ligand [compounds $Ru(acac)_3$ and $Ru(thd)_3$, respectively] causes the volatility to increase by two orders of magnitude in the temperature range from 104 to 120 °C (see Fig. 8). Based on the $P-T$ curves, the volatility series of ruthenium(III) β-diketonates (at $P = 10^{-3}$ Torr) is as follows:[98]

$Ru(hfac)_3$ (19 °C) > $Ru(ptac)_3$ (49 °C) > $Ru(tfac)_3$ (mixture of isomers) (75 °C) > $Ru(thdF)_3$ (84 °C) > > $Ru(thd)_3$ (91 °C) > $Ru(acac)_3$ (129 °C)

A comparison of the volatilities of ruthenium(III) β-diketonates showed[98] that replacement of terminal substituents in the β-diketonate ligands may cause the vapour pressures of compounds at the same temperature to change by nearly 5 orders of magnitude.

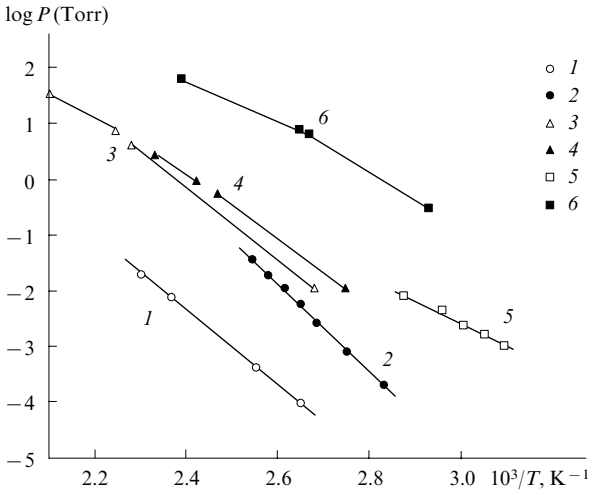


Figure 8. $P-T$ plots for ruthenium(III) β-diketonates.[98] $Ru(acac)_3$ (*1*), $Ru(thd)_3$ (*2*), *trans*-$Ru(tfac)_3$ (*3*), *cis*-$Ru(tfac)_3$ (*4*), $Ru(ptac)_3$ (*5*) and $Ru(hfac)_3$ (*6*).

There are only two publications[47, 84] concerning high-temperature mass spectrometric studies of vapour-phase thermolysis of the complexes $Ru(acac)_3$ and $Ru(tfac)_3$. Their authors proposed possible mechanisms of molecular decomposition on the heated surface involving intramolecular decomposition to HL and organic fragments.

An analysis of high-temperature mass spectrometry data for $Ru(acac)_3$ showed that in a vacuum in the temperature range from 210 to 350 °C the major volatile by-products (HL) of thermal decomposition are as follows:

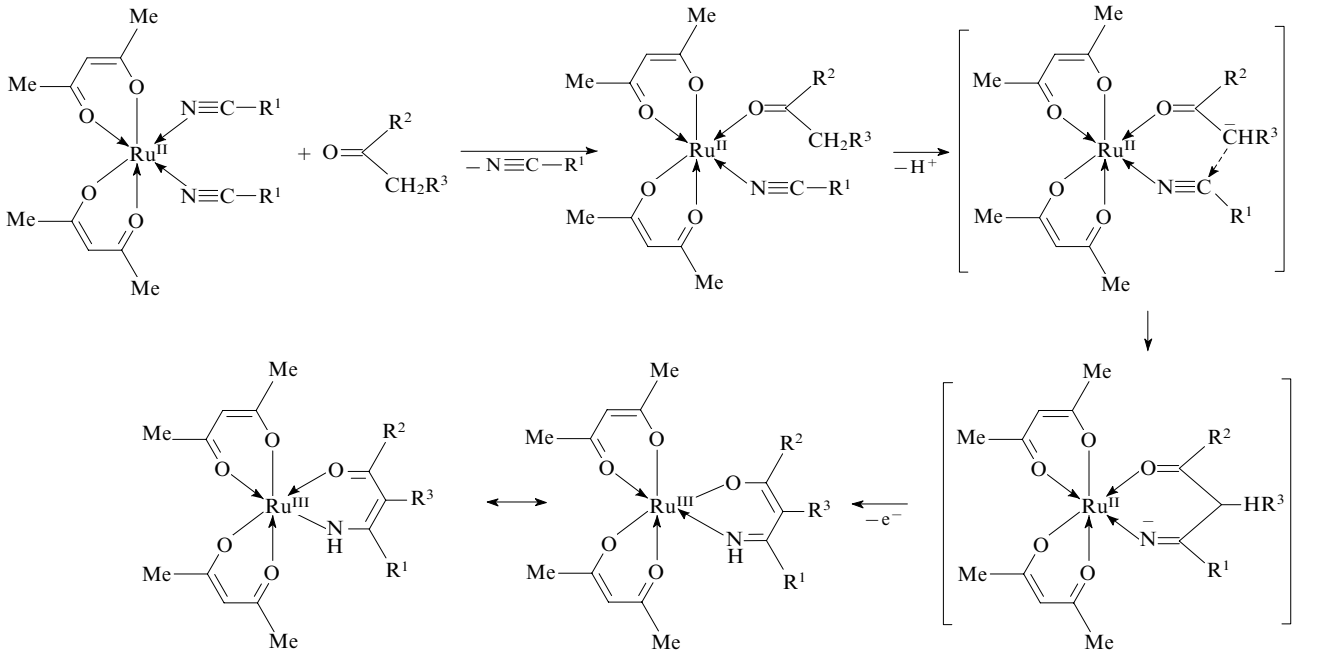
L	acac	Me	COC_2H_3	COMe	COCH	CO	COC_2H_4
$m:z$	100	84	55	43	41	28	56

At >350 °C, by-products of acetylacetone decomposition appear. Taking into account this fact, it was concluded that ruthenium films deposited from $Ru(acac)_3$ using no reagent gases will be characterized by a high content of impurities of carbon-containing fragments. In the presence of deuterium in the reaction zone, the major volatile by-product of $Ru(acac)_3$ decomposition will be only acetylacetone with different content of hydrogen and deuterium atoms. No other organic products were detected at a level of sensitivity of the mass spectrometric equipment.[47] Based on this fact, it was concluded that in the presence of hydrogen in the reaction zone almost carbon-free ruthenium films can be obtained in the temperature range 210–350 °C.

A study of thermal decomposition of $Ru(acac)_3$ vapours in the presence of oxygen showed that the vapours are unstable at 170 °C. Major volatile by-products of the process below 350 °C include acetylacetone and CO_2.

Thermolysis of $Ru(tfac)_3$ vapours in a vacuum begins at a higher temperature (490 °C). It follows that the thermal stability of vapours of ruthenium(III) β-diketonates increases upon introduction of fluorine-containing substituents into the ligand.[84] Thus, fluorinated ruthenium(III)

Scheme 1



β-diketonates characterized by higher vapour pressure and thermal stability are appropriate for being used as precursors in MOCVD processes. However, in this case the vapour phase can contain fluorine-containing fragments and high temperatures are required for thermolysis of the vapours. This makes fluorinated ruthenium(III) β-diketonates of limited use; however, it is noteworthy that $Ru(acac)_3$ is suitable for deposition of carbon-free ruthenium films in the presence of hydrogen.[47]

Six new hetero-ligand complexes of ruthenium(III) with the general formula $Ru(acac)_2L$ were synthesized by reactions of ketones (acetone, methyl ethyl ketone, monochloroacetone and acetylacetone) with ruthenium(II)complexes, $[Ru(acac)_2(AN)_2]$ or $[Ru(acac)_2(BN)_2]$ (AN is acetonitrile and BN is benzonitrile) following Scheme 1.[99]

One of these six complexes is structurally similar to $Ru(acac)_3$. Therefore, one can assume that such compounds can be highly volatile and thermally stable, thus being precursors for utilization in MOCVD processes.

5. Ruthenium(II) cyclopentadienyl derivatives

Metal cyclopentadienyl complexes are synthesized by reactions of alkali metal, magnesium or thallium cyclopentadienyls with corresponding metal salts and by reactions of cyclopentadiene with metal halides in the presence of bases.[100] Ruthenocenes belong to the most widely used precursors for MOCVD synthesis of ruthenium films that are produced on a large scale. Complexes are synthesized in inert atmosphere by reactions of $RuCl_3$ or $RuOHCl_3$ with appropriate sources of ligands (usually, HCp, HCp′, HEtCp, HPr^iCp) in ethylene glycol or ethanol in the presence of zinc dust as reducing agent. The yield of the final product can be as high as 80%.[28]

White crystals of the complex $Ru(Cp)_2$ with $T_m = 199-200$ °C are stable in air, readily soluble in nonpolar solvents and in most polar solvents without decomposition; $Ru(Cp)_2$ is synthesized by reaction of $[Ru(cod)Cl_2]_x$ with thallium cyclopentadienyl in dimethoxyethane in 78% yield.[101] An alternative synthetic route involves reactions of $[Ru(cod)Cl_2]_x$ with $[SnBu^n(R_5C_5)]$

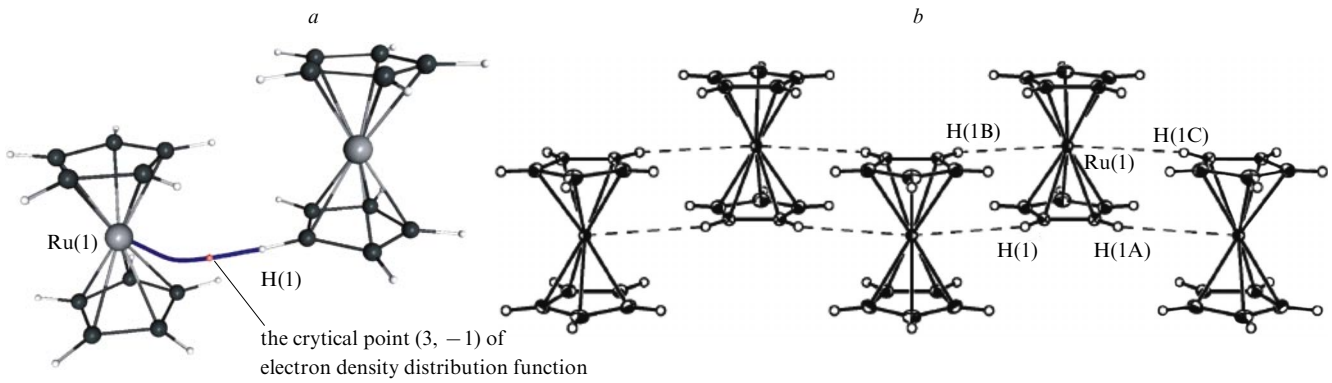


Figure 9. Molecular structure of $Ru(Cp)_2$, intermolecular contacts Ru···H (*a*) and molecular packing (linked Ru···H chains) in the crystal (*b*).[102]

Table 1. Selected properties of precursors of ruthenium(II) and ruthenium(III) complexes.

Compound	Molecular formula	Molecular mass	CAS [a] number	Physical properties			Temperature dependence of saturated vapour pressure	Ref.
				physical state	colour	T_m /°C		
$Ru(acac)_3$	$Ru(MeC(O)CHC(O)Me)_3$	398.40	14284-93-6	solid (powder)	red	240	$\log P$ (atm) = 25.56 − 15228/T (sublimation)	87, 94–98
trans-$Ru(tfac)_3$	$Ru(CF_3C(O)CHC(O)Me)_3$	560.33	16702-38-8	the same	"	171	$\log P$ (atm) = 28.78 − 14885/T (sublimation) $\log P$ (atm) = 16.99 − 9656/T (evaporation)	87, 94–98
cis-$Ru(tfac)_3$	$Ru(CF_3C(O)CHC(O)Me)_3$	560.33	16702-38-8	"	"	132	$\log P$ (atm) = 27.52 − 14076/T (sublimation) $\log P$ (atm) = 20.41 − 11202/T (evaporation)	87, 94–98
$Ru(hfac)_3$	$Ru(CF_3C(O)CHC(O)CF_3)_3$	722.26	16827-63-7	"	"	100	$\log P$ (atm) = 26.40 − 11665/T (sublimation) $\log P$ (atm) = 17.00 − 8145/T (evaporation)	87, 94–98
$Ru(thd)_3$	$Ru(Bu^tC(O)CHC(O)Bu^t)_3$	650.88	38625-54-6	"	orange	141	$\log P$ (atm) = 35.70 − 17920/T (sublimation)	87, 94–98
$Ru(ptac)_3$	$Ru(Bu^tC(O)CHC(O)CF_3)_3$	686.57	–	liquid	red	–	$\log P$ (atm) = 14.80 − 9110/T (evaporation)	87, 94–98
$Ru(dtc)_3$	$Ru(Et_2NCS_2)_3$	545.88	–	solid (powder)	"	232	$\log P$ (atm) = 34.60 − 22284/T (sublimation)	87
Ru $(allyl)_2(nbd)$	$Ru(C_7H_8)(C_3H_5)_2$	275.07	–	the same	white	108	$\log P$ (atm) = 15.90 − 8643/T (sublimation)	27, 87
Ru $(allyl)_2(cod)$	$Ru(C_8H_{12})(C_3H_5)_2$	291.07	–	"	"	99	$\log P$ (atm) = 15.01 − 8742/T (sublimation)	27, 87
$Ru(Cp)_2$	$Ru(C_5H_5)_2$	231.26	1287-13-4	"	"	199	$\log P$ (Torr) = 13.70 − 5170/T (sublimation)	87, 95, 101, 102
$Ru(EtCp)_2$	$Ru(EtC_5H_4)_2$	287.37	32992-96-4	liquid	yellow	–	$P \approx 0.25$ Torr at 85 °C and ~10 Torr at 120 °C	87
$Ru(dmpd)_2$	$Ru(Me_2C_5H_3)_2$	291.43	85908-78-7	solid (powder)		85	$\log P$ (Torr) = 8.619 − 3502/T	87
$Ru(Pr^iCp)_2$	$Ru(Pr^iC_5H_4)_2$	315.45	–	liquid	"	115–135	$\log P$ (Torr) = 5.6004 − 263.7/T (evaporation)	87
$Ru(thd)_2(cod)$	$Ru(Bu^tC(O)CHC(O)Bu^t)_2(C_8H_{12})$	575.80	329735-79-7	solid (powder)	yellow-orange	188	–	49, 50
$Ru_3(CO)_{12}$	$Ru_3(CO)_{12}$	639.34	15243-33-1	the same	orange	150	$\log P$ (Torr) = 13 − 5490/T (sublimation)	85–87
$Ru(CO)_3(chd)$	$Ru(CO)_3(C_6H_8)$	241.16	–	liquid	bright yellow	–	P = 0.28–5 Torr in the temperature range from 5 to 0 °C (evaluation)	32, 33

[a] CAS stands for Chemical Absracts Service.

(R = H, Me) in ethanol at 80 °C (yields are 75% and 70%, respectively). An analysis of the molecular packing of $Ru(Cp)_2$ in the crystal (Fig. 9) revealed [102] a shorter distance between the ruthenium atom and the Cp ligand of adjacent molecule compared to other metallocenes (*e.g.*, iron and nickel) as well as intermolecular contacts Ru···H that favour an approach of adjacent molecules and make rotation of Cp rings hindered, thus making the structure of the compound more ordered (see Fig. 9 *b*).

Some methods of synthesis of non-symmetric ruthenocenes were reported.[103, 104] Reactions of $[Ru(Cp^*)Cl_2]$ with other cyclopentadienyl derivatives of alkali metals and their analogues result in non-symmetric ruthenocenes [104] with cyclopentadienyl, indenyl, fluorenyl, acetylcyclopentadienyl and pentachlorocyclopentadienyl ligands. Information on thermal properties of the most often used precursors, *viz.*, $Ru(Cp)_2$, $Ru(EtCp)_2$ and $Ru(Pr^iCp)_2$, is scarce.

Complex $Ru(Cp)_2$ sublimes without decomposition on heating in N_2 + 5% H_2 atmosphere; the TGA curve demonstrates a 100% mass loss (Fig. 10) in the temperature range 25–210 °C.[95] At present, the most promising and commercially available volatile ruthenium precursors are compounds with low melting points, namely, $Ru(Cp)_2$ and, *e.g.*, $Ru(EtCp)_2$, a yellow liquid having a vapour pressure of ~ 0.25 Torr at 85 °C and ~10 Torr at 120 °C.[87]

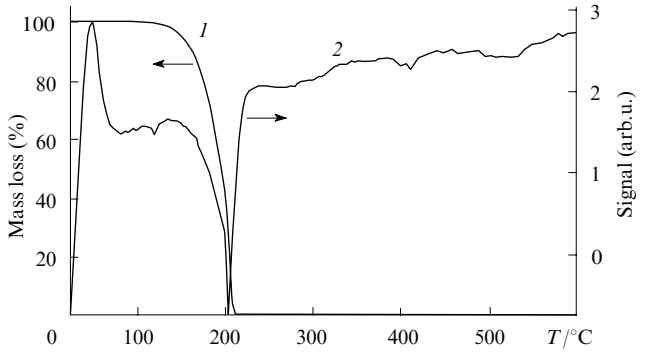


Figure 10. TGA (*1*) and DTA (*2*) curves of $Ru(Cp)_2$ heated in N_2 + 5% H_2 atmosphere.[95]

Numerical values of the vapour pressures of the cyclopentadienyl derivatives $Ru(dmpd)_2$ and $Ru(Pr^iCp)_2$ are available in the literature.[87] The $P-T$ plots for a number of ruthenium precursors from different classes of compounds are collected in Table 1 and in Fig. 5. As can be seen, by varying terminal substituents in ruthenium(III) β-diketonates one can span the entire range of changes in volatility for the most widely used (including commercially available) ruthenium precursors. This is indicative of predominance of the nature of the ligand used on the vapour pressure of a compound.

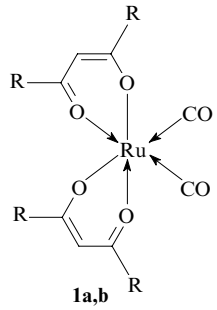
6. Other ruthenium precursors

Low-molecular-mass allylic derivatives of metals are highly volatile and can sublime from the reaction mixture at low temperatures; their stability increases upon introduction of other ligands, such as CO, Cp, halogen atoms, phosphines, *etc*. A number of hetero-ligand ruthenium(II) complexes were synthesized by reaction of allylmagnesium chloride (or allylmethylmagnesium chloride) with the polymer $[RuCl_2(cod)]_n$.[27] The reactions resulted in white crystalline complexes; the yields were at most 50%. The complexes were unstable in air, namely, their colour rapidly changed from white to dark-brown, the compounds dissolved in benzene and ether, were insoluble in ethanol and decomposed in chlorine-containing solvents.

Ruthenium trichloride hydrate reacts with cyclodienes in a solution in ethanol in inert atmosphere in the presence of metallic zinc to give cyclodienyl complexes of Ru(0) (Scheme 2).[105]

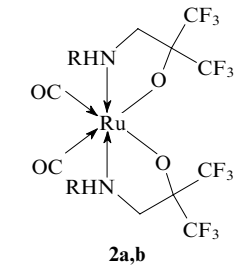
Complexes $[Ru(CO)_2(amak)_2]$ (**1**, **2**) and $[Ru(cod)(amak)_2]$ (**3**, **4**) were synthesized;[106] here, amak stands for a series of fluorinated aminoalkoxy ligands with the general formula $HOC(CF_3)_2CH_2NHR$ (R = H, Me, Et and $(CH_2)_2OMe$).

Structures 1–4



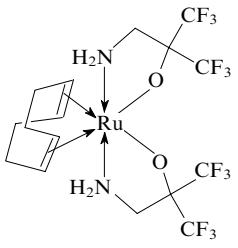
1a,b

R = CF_3 (**a**, $[Ru(CO)_2(hfac)_2]$), Bu^t (**b**, $[Ru(CO)_2(hmhd)_2]$)

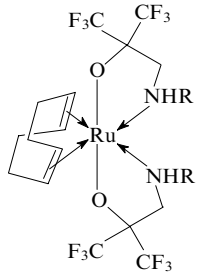


2a,b

R = H (**a**), Me (**b**)



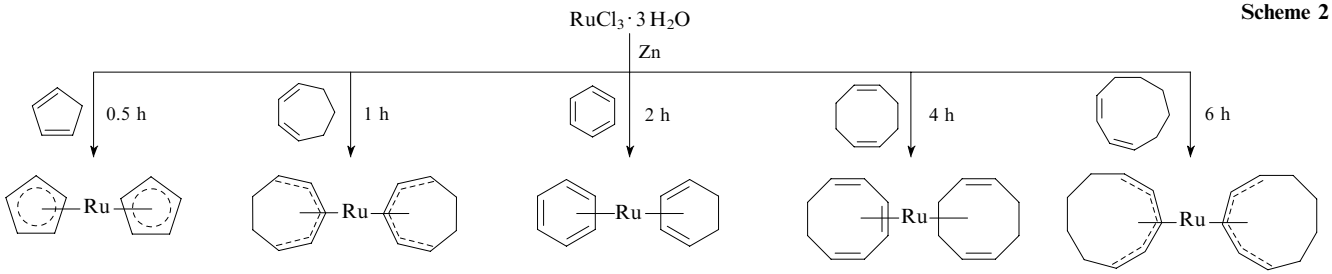
3



4a,b

R = Et (**a**), $(CH_2)_2OMe$ (**b**)

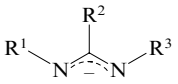
Scheme 2



The starting compounds were $Ru_3(CO)_{12}$ and $[Ru(cod)Cl_2]$; the reaction was carried in nitrogen atmosphere in the presence of hexane or tetrahydrofuran and sodium hydride. Structural parameters were determined for complexes **2a**, **3** and **4a**. These compounds are thermally stable and have a high vapour pressure.[106]

Novel amidinate ruthenium complexes **5** with the ligands R^1, R^2, $R^3 = H$, F, CF_3, *etc.*[106] were used in deposition of metallic ruthenium films.[107] Other data on thermal properties of these compounds are absent.

Structure 5



5

Thus, about thirty compounds of ruthenium in the low oxidation states (0, II, III) were studied as precursors for deposition of ruthenium-containing films. It was shown that the properties of compounds (volatility, thermal stability) depend primarily on the nature of the ligand. However, currently deposition of ruthenium-containing coatings by CVD is carried out using a small number of volatile compounds, namely, $Ru_3(CO)_{12}$, $Ru(CO)_3(chd)$, $Ru(Cp)_2$, $Ru_3(EtCp)_2$, $Ru(acac)_3$ and $Ru(thd)_3$. This is due to simple synthesis of these compounds, availability of the initial reactants, stability on storage and admissible thermal properties. Utilization of other precursors is limited by the absence of synthetic procedures with sufficiently high yields of the target compounds, high cost, instability during the synthesis and on storage (the need for inert atmosphere), and possible presence of halogen-containing fragments in the vapour phase when carrying out a MOCVD process. Also, many compounds contain large amounts of carbon atoms. In this connection, studies on the mechanisms of thermal decomposition of precursor vapours in the presence and in the absence of reactive additives (oxygen, hydrogen, other volatile reactants) become of crucial importance to targeted choice of reaction conditions.

IV. Ruthenium films

Data on the growth and properties of ruthenium films of different thickness (d) deposited from different precursors at different temperatures (T_d) and deposition rates (W) are collected in Table 2.

1. Ruthenium carbonyls and their derivatives

Ruthenium carbonyls and their derivatives were studied by few research groups. Deposition from the base precursor $Ru_3(CO)_{12}$ in the presence of hydrogen and oxygen led to growth of only ruthenium films. At 300 °C, the films showed excellent adhesion to silicon substrate, a low resistance and were almost carbon-free.[3]

The main method of modification of $Ru_3(CO)_{12}$ is to replace a number of carbonyl groups by some other groups. This enables stabilization of molecules (thermal decomposition temperature increases) and transition from $Ru_3(CO)_{12}$ powder to liquid hetero-ligand compounds that are much more convenient for practical implementation of the process. The most appropriate complex, $Ru(chd)(CO)_3$,[33,34] was studied by two research groups. No nucleation delay at relatively high temperatures (> 300 °C) was reported;[35] the deposition rate was as high as 20 nm min^{-1} and the specific resistance of the ruthenium film was 11–15 μΩ cm; however, the coatings contained rather high concentrations of carbon.

A series of publications concerning practical implementation of the ALD regime using the same precursor was reported.[36–44] This seems to be the most comprehensive and multi-factor investigation of regularities of the growth of ruthenium films, carried out in a wide range of deposition parameters. Also, in contrast to most publications of other authors, the design and operation of the PMOCVD machine were reported in detail.[39] This information is necessary to test the methodology of the process, in particular, for correct choice of the duration of reactant pulses and purge gas (argon).

Ruthenium was deposited on different materials, namely, Si, SiO_2, Al_2O_3, HfO_2, Si_3N_4, TiN including wafers coated with sputtered subnanometre-thick seed films of platinum group metals (Pt, PtPd, Ru) or their alloys. Parameters of the experiments were varied over wide ranges. Three-dimensional structures based on ~0.75 μm-thick silica film grown on silicon were used. The structures represented long grooves ~0.3 μm wide or holes ~0.3 μm in diameter that formed after anisotropic plasma etching in a silica film (upon completion of etching on silicon). The 3D structures were characterized by an aspect ratio (see Fig. 1 *b*) of ~2.5.

Deposition of ruthenium on insulators at low temperatures (< 200 °C) was accompanied by long nucleation delays that disappeared at temperatures above 200 °C. At low temperatures, polycrystalline and coarse-grained ruthenium films formed (Fig. 11 *a–c*), with ruthenium nuclei on the wafer surface serving as coating growth centres; usually, no continuous films are formed. At high deposition temperatures, one deals with more uniform formation of ruthenium nuclei on the surface and growth of fine-grained polycrystalline thick films (Fig. 11 *d–f*). This pattern is typical of the growth of ruthenium films (also, using other precursors), being indicative of nucleation in the vapour phase at high temperatures.

Photomicrographs of deposited ruthenium grains are shown in Fig. 12 *a–c*. Clearly, such a character of the growth of ruthenium films contradicts the idea of ALD growth that implies layer-by-layer formation of coatings.

However, when growth of fine-grained ruthenium nuclei at higher temperatures was followed by a decrease in temperature and subsequent growth of layers of necessary thickness at low temperatures (at, *e.g.*, 198 °C) and especially when Ru films were deposited on sputtered subnanometre films of platinum group metals and their alloys (Pd, PtPd, Ru), no nucleation delay was observed even at $T_d \approx 110$ °C. The Ru films had a fine-grained structure with a grain size of about 5 nm and coatings deposited on 3D structures were conformal (see Fig. 12 *d–f*).[36,37,41]

The authors of these publications also carried out detailed studies of the kinetics of layer growth (including 3D structures; this is of importance for practical applications of ruthenium in micro- and nanoelectronics), of the structure and properties of films deposited under different conditions and after continuous and pulsed thermal annealing. The compositions of the layers grown using different deposition regimes were investigated by secondary ion mass spectrometry. A number of growth schemes for ruthenium films under different conditions were proposed.

Table 2. Selected data on the growth, structure, chemical composition and properties of polycrystalline ruthenium films prepared by different CVD techniques.

Method	Precursor	Second reactant	Substrate	T_d /°C	ND [a]	W [b]	d /nm	Film composition	Grain size /nm	Grain orientation	Carbon content in the film (at.%)	ρ /μΩ cm	Ref.
Different complexes													
MOCVD	$Ru_3(CO)_{12}$	–	Si	250–400	–	–	100–250	Ru	30	(100)	0	17	3
	$Ru(acac)_3$	–	SiO_2	500	–	–	100–250	Ru	10–40	–	60	1940	3
	$Ru_3(CO)_{12}$	H_2, O_2	Si, SiO_2	250–400	–	–	100–250	Ru	–	–	–	–	3
	$Ru(Cp)_2$	O_2	Si, SiO_2	600	–	–	100–250	Ru/RuO_2	50–75	(200), (111)RuO_2	< 20	14.8	3
	$Ru(Cp)_2$	O_2	Si	575	–	–	100–250	RuO_2	500	–	< 20	89.9	3
	$Ru(acac)_3$	H_2	Si, SiO_2	500	–	–	100–250	Ru	–	–	–	–	3
	$Ru(acac)_3$	O_2	Si, SiO_2	500	–	–	100–250	Ru	–	–	–	–	3
	$Ru(acac)_3$	H_2	Si	600	–	–	100–250	Ru/RuO_2	30–100	(002)Ru	0	521	3
	$Ru(acac)_3$	O_2	Si	600	–	–	100–250	RuO_2	10–50	–	< 20	643	3
Ruthenium carbonyl derivatives													
MOCVD	$Ru(chd)(CO)_3$	N_2O	SiO_2	210	–	14.7	–	Ru	–	–	–	138	33
	$Ru(chd)(CO)_3$	N_2O	SiO_2	210	–	7.2	–	Ru	–	–	–	108	
	$Ru(chd)(CO)_3$	N_2O	Si	190	–	–	170	Ru	–	–	–	–	34
	$Ru(chd)(CO)_3$	N_2O	Si, SiO_2, Al_2O_3	150–460	–	2–19	–	Ru	14–300	–	~ 7.5	21–11	35
PMOCVD	$Ru(chd)(CO)_3$	N_2O	Si, SiO_2, Al_2O_3, HfO_2, Si_3N_4	110–350	ND	0.1–12	< 100	Ru	5–70	(111), (102)	14 mass %–20 mass % (180–260 °C)	~ 15 (200 °C)	36–44
	$Ru(chd)(CO)_3$	NH_3, N_2O, H_2	PtPd, Ru, Pt	110–260	no ND	0.1–0.5	< 45	Ru	~ 5	–	–	–	36–44
Ruthenium β-diketonates													
PMOCVD	$Ru(acac)_3$	O_2	SiO_2/Si	300–450	–	0.2–1.6	< 20	Ru	–	(002)	–	15.1–11.5	46
	$Ru(acac)_3$	H_2	SiO_2/Si	300–370	–	0.002–0.007	5–25	Ru	3–4	–	–	–	47
	$Ru(thd)_3$	O_2	SiO_2/Si	110–350	–	2–9	to 80	Ru	–	(100), (002), (101), (102), (110), (103)	see [c]	400 (1% O_2) 100 (10% O_2) 30 (50% O_2)	48 48 48
	$Ru(thd)_2(cod)$	O_2	SiO_2/Si	400–480	–	3–5	–	Ru	–	(100), (002), (101), (102)	< 5	47	49
	$Ru(thd)_2(cod)$	H_2	SiO_2/Si	430–450	–	< 1	–	Ru + RuO_x		–	–	–	618
49													
PACVD	$Ru(thd)_2(cod)$	O_2	SiO_2/Si	330–450	–	0.7–5	–	Ru	–	(100, 002, 101, 102)	–	~ 70	49
	$Ru(thd)_2(cod)$	H_2	SiO_2/Si	330–450	–	–	–	Ru	–	–	see [c]	> 1000	49
PMOCVD	$Ru(thd)_2(cod)$	O_2	HfO_2/Si	280–320	–	–	14–20	Ru–RuO_x	–	–	–	20.6	50
	$Ru(thd)_3$	O_2	Al_2O_3	325–460	–	0.036	–	Ru	–	–	< 1.9 at.% C, < 2.9 at.% H, < 5.5 at.% O	20	51
	$Ru(thd)_3$	O_2	SiO_2/Si	225–400	–	–	3–10	Ru	–	(002)	1.5	~ 100–200	52

Table 2 (continued).

Method	Precursor	Second reactant	Substrate	T_d /°C	ND [a]	W [b]	d/nm	Film composition	Grain size /nm	Grain orientation	Carbon content in the film (at.%)	ρ /μΩ cm	Ref.
Ruthenocene and its derivatives													
MOCVD	$Ru(Cp)_2$	H_2	Pt/SiO_2	⩽177	see [d]			Ru	–	–	–	–	53
				>177	see [e]			Ru	–	–	–	–	53
PMOCVD	$Ru(Cp)_2$	O_2	Al_2O_3, TiO_2	275–400	–	–	–	Ru	–	(002)	low	20	20
	$Ru(Cp)_2$	O_2	Ru	350	–	0.045	–	Ru	–	–	–	–	54
	$Ru(Cp)_2$	O_2	Al_2O_3	>275	ND	0.023	–	Ru	–	(101)	–	–	55
			Ir	>225	–	0.035	–	Ru	–		–	–	55
	$Ru(thd)_3$	O_2	Al_2O_3	>325	–	0.033	–	Ru	–				55
			Ir	>250	–	0.015	–	Ru	–	(101), (002)	–	–	55
	$Ru(Cp)_2$	O_2	HfO_2, SiO_2, Si–H	325	maximum ND for Si–H	0.1	>15	Ru	–	(002), (101)	low	–	56
	$Ru(Cp)_2$	O_2	Si, SiO_2,	300	ND	0.09	–	Ru	–	(002), (101)		25–40	57
	$Ru(EtCp)_2$	O_2	TaN_x, Ta_2O_5										
PACVD	$Ru(Cp)_2$	NH_3	Si, SiO_2,	300	no ND	0.08	–	Ru	–	(002), (101)		25–40	57
	$Ru(EtCp)_2$	NH_3	TaN_x, Ta_2O_5										
PMOCVD	$Ru(Cp)_2$	O_2	Si, SiO_2, Ta_2O_5	300–350	–	0.12	~35	Ru	–	(101), (002)		11	58
MOCVD	$Ru(Cp)(Pr^iEt)$	O_2	Si, SiO_2, TiN, Ta_2O_5	300–400	see [f]	16–24	< 100	Ru	–	(101), (002), (100)	–	12	59
	$Ru(EtCp)_2$	O_2	Si, SiO_2	300–400	–	20	20	Ru	–	(101), (100)	low	12	61
	$Ru(EtCp)_2$	O_2	3D substrate	280–360	–	6	–	Ru,	–	(100), (101)	20–30	–	13
			coated with a Ta_2O_5 layer	320	conformality 60%–90%			RuO_2	–	(110), (101), (200), (211)	–	–	13
	$Ru(EtCp)_2$	O_2 (1.3 and 25%)	SiO_2/Si	200-400	ND depends on $[O_2]$ and T_d	10–30	100–300	Ru	–	(101), (002)	$[C] \approx 10^{19}$, $[O] \approx 10^{21}$ atm cm^{-3}	8–150	62, 63
PMOCVD	$Ru(EtCp)_2$	O_2	TiN	270	ND	0.15	20	Ru	–	(002), (101)	< 2	15	7
PACVD	$Ru(EtCp)_2$	NH_3	TiN	270	–	0.038	–	Ru	–	(002), (101)	–	12	21, 22
	$Ru(EtCp)_2$	NH_3	SiO_2	300	–	–	–	Ru	–	–	–	–	66
MOCVD	$Ru(EtCp)_2$		SiO_2	260–500	ND	–	–	Ru	150	(101), (002)	–	15–20	67, 68
	$Ru(EtCp)(dmpd)$		SiO_2	260–500	short ND	–	–	Ru	50	(002), (101)	–		67, 68
PMOCVD	$Ru(EtCp)(dmpd)$	O_2	Si, SiO_2, TiO_2, TiN	230–280	–	0.04	–	Ru	–	(002), (101)	–	19	25, 69
MOCVD	$Ru(dmpd)_2$	O_2	SiO_2	220–400	–	0.3	–	Ru	–	(002)	–	~10–140	70, 71

Table 2 (continued).

Method	Precursor	Second reactant	Substrate	T_d /°C	ND [a]	W [b]	d/nm	Film composition	Grain size /nm	Grain orientation	Carbon content in the film (at.%)	ρ /μΩ cm	Ref.
Other precursors													
MOCVD	$[Ru(Cp)(CO)_2]_2$	O_2	BST, Si_3N_4	25–600	–	–	1–100	Ru	–	–	low	28	45
	RuO_4	H_2	Si, SiO_2, SiC, TiN, HfO_2, Ta, TaN	150–200	–	1.5	–	Ru	–	(002), (101)		20	72, 73
PMOCVD	RuO_4	H_2	Si_3N_4, La_2O_3, Al_2O_3, Ta_2O_5	150–200	no ND on TiN	0.43	–	Ru	–	the same	"	"	72, 73
	$Ru(Bu^tMe\text{-}amd)_2(CO)_2$		SiO_2, WN	200–300	no ND	0.04	2–8	Ru	5–20	(101), (100)	"	30–90	75
	IMBCHRu	O_2	TiN	220		0.1	10–20	Ru	–	–		36	77
			SiO_2	"	ND	0.086	10–20	Ru	–	–	"	"	77
PACVD	IMBCHRu	NH_3	TiN, SiO_2	225 (140–400)	no ND	0.094	10–70	Ru	12–20	(101), (002)	"	12	78

[a] Nucleation delay. [b] Film growth rates are given in nm min^{-1} for MOCVD processes and in nm per cycle for PMOCVD and PACVD processes. [c] The presence of carbon was assumed but its content was not estimated. [d] Selective growth of ruthenium on platinum. [e] Nonselective growth in a reactor. [f] Nucleation delay increased in the order $Ta_2O_5 < TiN < Si < SiO_2$.

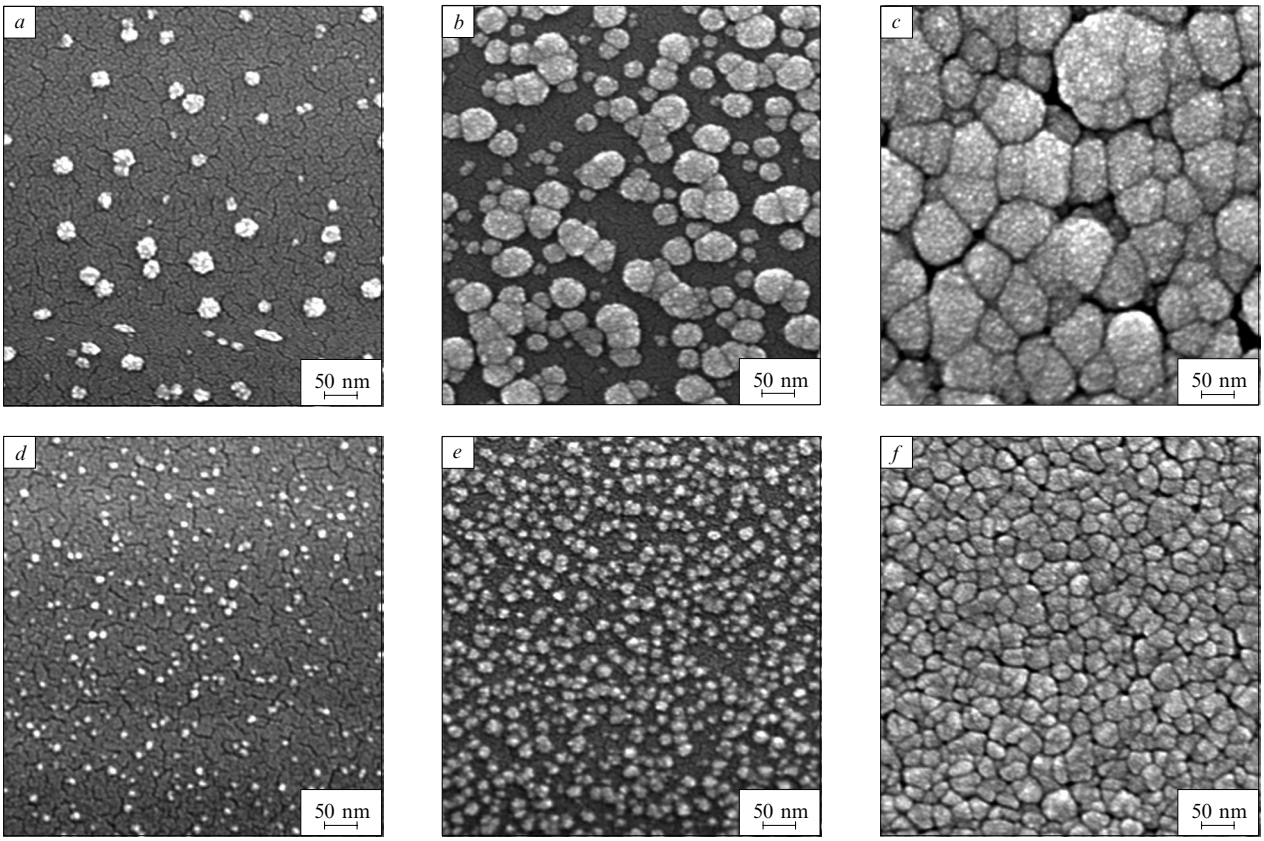


Figure 11. Photomicrographs of ruthenium films prepared at 198 (*a*–*c*) and 290°C (*d*–*f*) by PMOCVD from $Ru(chd)(CO)_3$ with N_2O as the second reactant.[37]
Number of deposition cycles: 50 (*a*), 100 (*b*), 300 (*c*), 1 (*d*), 10 (*e*) and 200 (*f*).

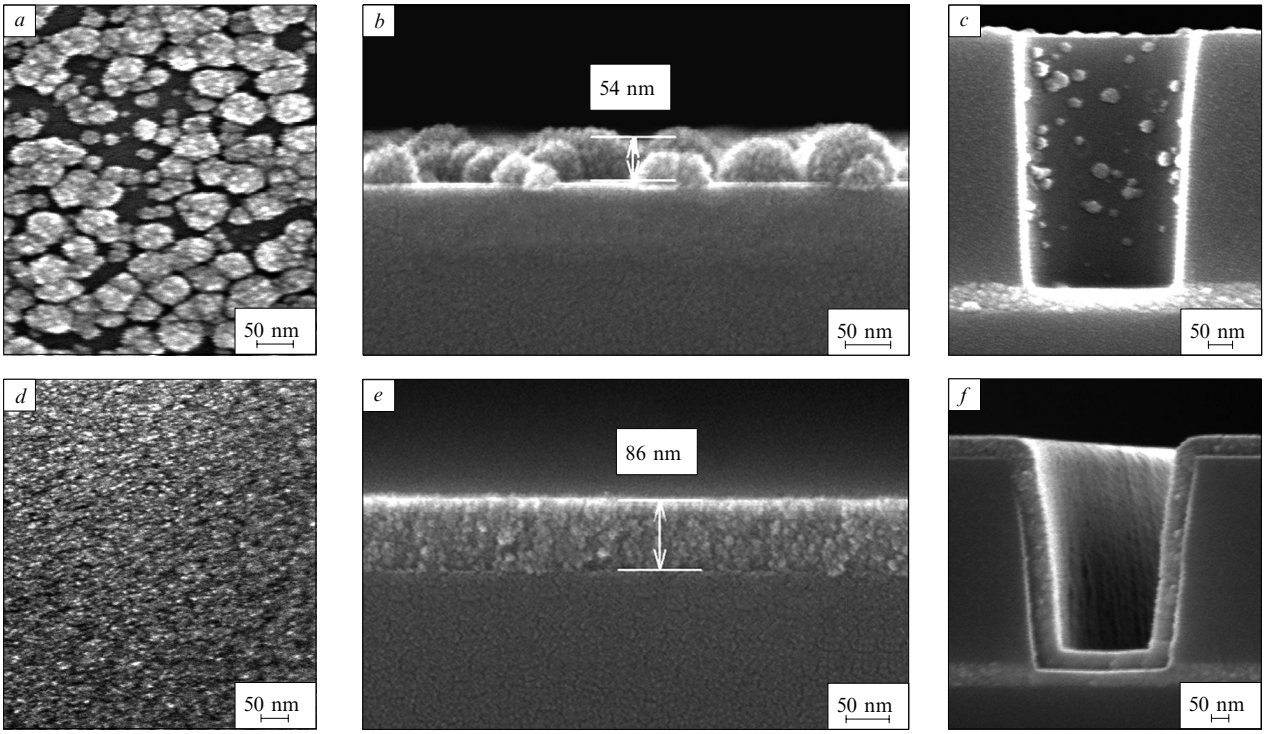


Figure 12. Photomicrographs of ruthenium films grown on SiO_2/Si (*a*,[37] *b*,[40] *c*[36]) and on PtPd/SiO_2/Si (*d*,[36] *e*,[40] *f*[36]).
Top view (*a*, *d*), cross section of ruthenium layer on the substrate surface (*b*, *e*) and cross sections of 3D structures (*c*, *f*). The subnanometre-thick PtPd seed film was sputtered on SiO_2 surface.

The best (from the standpoint of deposition and electrical resistance of ruthenium films) results were obtained using N_2O as co-reactant at deposition temperatures of about 200 °C. Conformal films on 3D structures were obtained only using seed films of platinum group metals; otherwise, only individual Ru grains were observed in the trenches; the grain concentration and size reduced with the trench depth (Fig. 12 *c*). High (relative to bulk) electrical resistance of ruthenium films is due to the presence of carbon impurity and, as a consequence, reduced density of ruthenium films upon deposition.

2. Ruthenium β-diketonates

Ruthenium coatings deposited by MOCVD from $Ru(acac)_3$ are of poor quality because they peel off the substrate, contain large amounts of carbon and have a high electrical resistance.[3] Films prepared at a higher deposition temperature (600 °C) in the presence of hydrogen contained ruthenium and ruthenium oxide phases (no carbon was detected), whereas films prepared using oxygen represented a RuO_2 phase containing up to 20 at.% of carbon.

The same precursor, $Ru(acac)_3$, was used in PMOCVD studies[46, 47] aimed at determining the ALD growth parameters. In one study,[46] portions of the precursor [including $Ru(acac)_3$ dissolved in octane] were periodically sprayed into a reactor; also, oxygen was continuously fed to the reactor using a separate line. The density of films with a surface roughness of about 1 nm was 11.7–12.7 g cm^{-3} according to X-ray diffraction data, being close to the density of bulk material (12.3 g cm^{-3}). However, trace amounts of ruthenia phase were detected on the surface films. In addition, ruthenia was present in the region of ruthenium/silica interface. Regularities of layer growth in 3D structures with an aspect ratio of 10, a diameter of 0.5 μm and 5 μm in depth were also investigated for different deposition regimes.[46] It was found that the degree of conformality decreases from 70% to 10% as the deposition temperature increases from 300 to 340 °C. Also, the degree of conformality decreased from 90% to 70% as the pulse duration decreased from 1.0 to 0.2 Hz at 320 °C.

A publication concerned with interdisciplinary approach to studies on the regularities of the growth of metallic ruthenium films from $Ru(acac)_3$ by PMOCVD using hydrogen as co-reactant is available.[47] It also includes the description of reaction intermediates detected *in situ* by high-temperature mass spectrometry. High-resolution TEM images of the cross-section of a Ru/Si structure are shown in Fig. 13. The film is composed of ruthenium crystallites ~3–4 nm in size and has a roughness similar to that of the initial Si/SiO_2 substrate (~1 nm).

In yet another study[48] metallic ruthenium films were deposited from $Ru(thd)_3$ dissolved in tetrahydrofuran; oxygen was used as reagent gas. The authors assumed that the nucleation delay can be minimized; this was confirmed by nearly linear plots of the deposition rate *vs.* time. At temperatures above 300 °C, the growth rate curves showed attainment of saturation. The deposition rate and the reciprocal dependence of the degree of conformality (in trenches 80 nm in diameter and 800 nm in depth, *i.e.*, at an aspect ratio of 10) were strongly dependent on the oxygen concentration (c_{O_2}) in the mixture.

c_{O_2} (%)	1	10	50
W/nm min^{-1}	2	5	9
Degree of conformality (%)	90	65	20

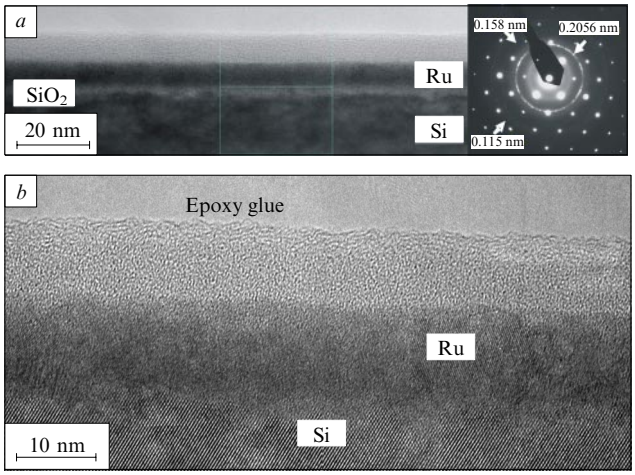


Figure 13. TEM image of the cross section of a ruthenium film deposited by PMOCVD from $Ru(acac)_3$ on SiO_2/Si substrate in the presence of H_2 at 340 °C and a gas-phase electron diffraction pattern of this film (interplanar spacings of 0.2056; 0.158; 0.115 nm correspond to hexagonal ruthenium lattice) (*a*) and a high-resolution TEM image of the film cross section (*b*).[47]

Polycrystalline ruthenium films prepared[51, 52] by PMOCVD from $Ru(thd)_3$ in the presence of oxygen as co-reactant were characterized by low content of impurities, but the growth rate was very low. The vapour phase composition was analyzed *in situ* by quadrupole mass spectrometry. The optimal deposition temperature was reported to be 300 °C[52] because below 260 °C, the deposition rate was inadmissibly low, while above 320 °C, the film roughness was very high. However, ruthenium films grown under optimal deposition conditions had rather high specific resistance (~100–200 μΩ cm). To reduce the specific resistance, a two-step technique was used, namely, deposition onto a seed layer under optimal conditions was followed by the deposition at elevated temperature; the specific resistance of the films thus prepared was in the range 8.6–14 μΩ cm.

Film deposition from $Ru(thd)_2(cod)$ precursor was also reported.[49, 50] The former study was carried out using thermally activated MOCVD process in a diode reactor and a mixture of the precursor with oxygen and hydrogen. In the latter case,[50] ruthenium films were grown in a PMOCVD reactor using the precursor dissolved in tetrahydrofuran and oxygen. Interestingly, an increase in the microwave plasma-activation power led to growth of oxide films with high electrical resistance. The PMOCVD study[50] was aimed at searching the ALD conditions, but attempts to detect relevant indications failed. Ruthenium films had a polycrystalline structure, carbon was detected only on the film surface. Also, the films contained up to ~ 13 at.% of oxygen according to Rutherford backscattering data. Differences between the electrical resistance of the films and that of bulk ruthenium was explained by the presence of RuO_x oxides on the ruthenium grain boundaries and at the interface between the deposited film and HfO_2.

3. Ruthenocene and its derivatives

Ruthenocene and its derivatives have been studied most intensively. This is probably due to the fact that $Ru(Cp)_2$ is

a commercially available, high-purity chemical for production of microelectronic devices. Initially, experiments with $Ru(Cp)_2$ were carried out. Subsequent changes in hardware and additional requirements for precursors (high fusibility or liquid state) in large-scale production of integrated circuits gave an impetus to modification of $Ru(Cp)_2$ by replacement of one or both cyclopentadienyl groups. Consider the main results of these investigations.

The possibility of fabrication of ruthenium films by MOCVD from $Ru(Cp)_2$ and oxygen at ~ 500 °C was for the first time demonstrated by Green *et al.*[3] At low deposition temperatures (below 177 °C), selective growth of ruthenium particles on the surface of a platinum gauze placed in a reactor was observed,[53] whereas no deposition on a quartz surface of the reactor walls occurred. An increase in temperature caused an identical growth of Ru films on the surfaces of all materials inside the reactor and on the platinum gauze.

A series of studies on the growth of ruthenium films by PMOCVD from $Ru(Cp)_2$ using oxygen was reported.[20, 54, 55] Polycrystalline ruthenium films grown on Al_2O_3 and TiO_2 substrates at 275–400 °C[20] were characterized by low content of impurities and a specific resistance of ~ 20 μΩ cm. The growth mechanism of ruthenium films and platinum films was studied by mass spectrometry and a quartz microbalance.[54] It was concluded that deposition is accompanied by partial oxidation of ligands that react with adsorbed oxygen to release CO_2 and H_2O. It is believed that reaction products remain on the surface and oxygen that is subsequently fed to the reaction zone is adsorbed on them. It was established that, depending on the experimental conditions, oxygen can faster or slower diffuse towards the near-surface region of the freshly deposited film and oxidize ligands without forming ruthenium oxide phases. Film deposition of platinum group metals including ruthenium was studied[55] by the PMOCVD method using $Ru(Cp)_2$ and oxygen, as well as $Ru(thd)_3$ and oxygen on Al_2O_3 and metallic iridium surfaces as seed layer in order to determine the lower limits of coating deposition temperatures for different surfaces. It was established that growth of ruthenium film on iridium surface occurs at much lower temperatures (see Table 2). This was interpreted as catalytic effect of iridium in the initial steps of the process. Taking into account this fact, deposition ruthenium on iridium surface with no nucleation delay is possible at much lower temperatures. The orientation of grains in the polycrystalline ruthenium film was precursor dependent.

Pulsed deposition of ruthenium[56] using $Ru(Cp)_2$ and oxygen on the surface of various substrates (SiO_2, HfO_2 and hydrogen-blocked silicon, Si–H) was studied *in situ* by Auger spectroscopy in order to establish correlations between the surface energy measured from the wetting angle. It was shown that the nucleation delay considerably increases as the wetting angle increases (a decrease in surface energy); the maximum wetting angle value was found for Si–H. The effect was explained by different concentrations of oxygen necessary for the reaction to proceed on different surfaces. Among these materials, hafnium dioxide was the most efficient for the growth of ruthenium film, because the rate of growth on HfO_2 was maximal owing to the presence of oxygen. Contrary to this, the Si–H surface appeared to be oxygen-deficient and had the highest concentration of carbon in the ruthenium film. It was also established that the grain orientation in the films depends on the type of the surface, *e.g.*, (101) on HfO_2 and (002) on SiO_2.

Metal-organic CVD of ruthenium films on TaSiN substrates (this material is used as diffusion barrier in fabrication of integrated circuits) was studied.[23] To enhance nucleation, the surface was treated with argon or hydrogen plasma or a palladium thin film was sputtered on the surface prior to ruthenium deposition from $Ru(EtCp)_2$. The last-mentioned technique gave the best results, *viz.*, the surface concentration of ruthenium nuclei appeared to be tens of times higher than that of Ru nuclei on the untreated TaSiN surface.

Ammonia plasma-activated PMOCVD of ruthenium from $Ru(Cp)_2$ and $Ru(EtCp)_2$ in oxygen atmosphere at 300 °C was reported.[57] No nucleation delay and no nitrogen was detected in the ruthenium films in the latter case. The authors emphasized the preferable orientation, (002), of ruthenium crystallites in the deposited films because such films used as, *e.g.*, the lower electrode in the MIM memory cell are appropriate for the formation of high-dielectric-constant-materials of the Ta_2O_5 type (see references cited in the original study). However, it should be noted that the activation step seems to be unpromising for deposition of conformal coatings on complex-shape structures with high aspect ratios, as required technologically for fabrication of memory cells for integrated circuits.[17]

The ideas of Aaltonen *et al.*[54] were developed by Park *et al.*,[58] who studied the dependence of pulsed growth of ruthenium films on the oxygen concentration that was varied by varying either pulse duration or partial pressure of oxygen at constant pulse duration. In the second case, the deposition rate appeared to be much higher and the deposited nanocrystalline ruthenium films contained an amorphous phase RuO_x, which led to an increase in the specific resistance of the films. The effect was explained by different concentrations of oxygen in the near-surface region attained using the two film growth methods. Namely, the oxygen concentration was much higher in the second case. Thus, the formation of the ruthenium oxide phase was primarily dependent on the partial pressure of oxygen rather than its dose.

Yet another MOCVD study[59] was carried out using $Ru(Cp)(Pr^iCp)$ as precursor and oxygen. It was established that $Ru(Cp)(Pr^iCp)$ makes it possible to prepare ruthenium films with the chemical composition and properties close to those of the films deposited from $Ru(Cp)_2$. The oxide phase in the ruthenium films was observed only at deposition temperatures above 400 °C and at high oxygen concentrations. Deposition on different thin film materials revealed the following drawbacks of ruthenium films:

— dependence of nucleation delay on the type of the surface material; the nucleation delay increased in the order

$$Ta_2O_5 < TiN < Si < SiO_2$$

— coarse-grained, polycrystalline structure of films with a surface roughness in the range from 3 to 6 nm.

Mechanical stress measurements of ruthenium films deposited on Si gave values ranging from 100 to 200 MPa at deposition temperatures above 350 °C and a value of 1000 MPa at 325 °C, which is inadmissible for memory cell technology.[59]

Next, a study[60] on the nucleation of ruthenium on different-type substrates including Si_3N_4, SiO_2, Ta_2O_5, TiN and TiO_2 revealed correlations with the type of chemical bonds in the substrate material. Namely, poor nucleation of ruthenium was observed for materials with covalent bonds (Si_3N_4, SiO_2, TiN); as a consequence, coarse-grained films formed. Also, growth of ruthenium oxide films on TiN was observed (*cf.* growth of ruthenium film on TiO_2). For better nucleation, the surface of the TiN (material for IC fabrication) was treated with argon plasma to remove nitrogen atoms from the near-surface region and, therefore, to change the properties of the surface and to stimulate growth of fine-grained ruthenium films. The best results were observed for nucleation on materials with ionic bonds, Ta_2O_5 and TiO_2, where continuous smooth ruthenium films formed.

Probably, liquid $Ru(EtCp)_2$,[7,21,22,61–66] has been best studied in this group of precursors. This allows one to simplify the feed line for $Ru(EtCp)_2$ vapours into reactors and to improve the reproducibility of deposition processes. As for $Ru(Cp)_2$, an important role is played by the oxygen to precursor vapour concentration ratio.

According to calculations,[61] oxygen is mainly consumed for ligand oxidation irrespective of the deposition temperature in the range from 250 to 500 °C. Depending on the deposition temperature, the minimum oxygen to $Ru(EtCp)_2$ vapour concentration ratios needed for full oxidation of ligands are as follows:

T/°C	250	350	400	500
O_2 : $Ru(EtCp)_2$	17	15	14	10

At $O_2 : Ru(EtCp)_2 > 18$, both ruthenium and ruthenium oxide phases should form simultaneously. Thus, according to calculations, the oxygen to precursor vapour concentration ratio can vary within a rather narrow range at low deposition temperatures (practically most valuable case). However, based on the tentative values of the sticking coefficients for oxygen and precursor vapour ($\sim$0.33 and $\sim$0.52, respectively), it was established that this ratio should be larger than the theoretical value. Since nucleation of ruthenium on the surface is possible when both reactants are available in a desired ratio, the experimental design should take into account the difference between the sticking coefficients.

The possibility for ruthenium films to grow from $Ru(EtCp)_2$ on 3D memory cell structures with good conformality was tested for three different IC sizes (0.13, 0.10 and 0.08 μm).[13] It was shown that the degree of conformality of the coatings (90%, 80% and 60%, respectively) reduced several-fold as the deposition temperature increased.

The growth kinetics of ruthenium films from $Ru(EtCp)_2$ in the presence of oxygen (1.3% and 25%) and the properties of these films were studied.[62,63] It was established that the nucleation delay reduced with increasing deposition temperature and oxygen concentration. The results obtained for an oxygen concentration of 1.3% are as follows:

ND/min	45	10	8	8	0
T/°C	220	230	240	270	300

At an oxygen concentration of 25%, the nucleation delay was 5 min at 230 °C. As the deposition temperature increased, the preferred grain orientation in the ruthenium films changed from (101) to (002). The films contained carbon ($\sim 10^{19}$ cm^{-3}) and oxygen ($\sim 10^{21}$ cm^{-3}) in the range of deposition temperatures from 240 to 270 °C. It was concluded that film growth is limited by the concentration of oxygen adsorbed on the surface of the growing ruthenium film. Under different experimental conditions the degree of conformality of the coating of the structures 0.4 μm wide and 0.7 μm deep considerably reduced with increasing deposition temperature above 230 °C and oxygen concentration in the mixture.

Similar results were obtained by other authors who studied the composition and properties of ruthenium films deposited from ruthenocene on Si, SiO_2/Si and TiO_2/SiO_2/Si substrates in the presence of oxygen in the temperature range 320–480 °C.[64,65]

Pulsed deposition of ruthenium from $Ru(EtCp)_2$ was reported.[7,21,22,66] Pulsed growth of a ruthenium film from $Ru(EtCp)_2$ with O_2 as co-reactant was studied[7] in order to utilize the ruthenium coating as seed layer for subsequent copper metallization: pulsed deposition on TiN surface was carried out at 270 °C. It was found that the composition of the Ru film can vary from Ru to RuO_2 depending on the ratio of the adsorbed reactants. The coating of steps on a structure with an aspect ratio of 8 and a diameter of 0.2 μm was characterized as perfect. However, we estimated the degree of conformality at $\sim$ 70%–80% based on the cross-section photographs of the structures (unfortunately, no experimental details were reported).

In a continuation of these studies Kwon *et al.*[21,22] proposed a PMOCVD technique using $Ru(EtCp)_2$ and plasma-activated ammonia as co-reactant (plasma was generated at a radiofrequency of 13.56 MHz). In this case, the growth rate of ruthenium films was 0.038 nm per cycle and no nucleation delay was observed. The preferred grain orientation was (002) and increased with increasing plasma discharge power [unlike the (101) orientation in the case of thermally activated pulsed growth from $Ru(EtCp)_2$ and oxygen]. The specific resistance of the films was 12 μΩ cm, the density was to 12.03 g cm^{-3}, the surface roughness was nearly 0.7 nm at a film thickness of 50 nm; no nitrogen and carbon impurities were detected.

The possibility of controlled growth of ruthenium nanocrystals 2.2–5.1 nm in size and their concentration of $(3.5–8) \times 10^{11}$ cm^{-2} on the substrate surface was studied.[66] The process conducted at 300 °C involved two steps, *viz.*, nucleation and growth that were controlled by varying various parameters. Film growth from a mixture of $Ru(EtCp)_2$ and plasma-activated ammonia initially led to slow formation of small, nearly same-size ruthenium nuclei. Thermal activation and the use of a mixture of $Ru(EtCp)_2$ with oxygen caused the growth rate of Ru nuclei to increase; the nuclei were characterized by a broad size distribution and their surface concentration was low. Film growth after nucleation to a necessary thickness of the coating occurred in the pulsed regime using thermally activated gas mixture. This approach enabled independent control of the density and size of ruthenium nanocrystallites on the substrate surface.

Preparation of ruthenium films from liquid precursors based on $Ru(EtCp)_2$ by MOCVD in nitrogen stream was investigated by researchers from Japan [67, 68] and South Korea [24, 25, 69] Both cases, with one and two EtCp moieties replaced by the dmpd group, were studied.[70, 71] A comparison of the durations of nucleation delays and the structures of the coatings prepared using $Ru(EtCp)_2$ and Ru(EtCp)(dmpd) revealed a considerable (several-fold) decrease in the duration of the nucleation delay in the latter case. Enhanced nucleation led to formation of more dense films and grain growth mainly occurred along the (002) direction. Of particular interest are the data on the conformality of the Ru films, which was 98%–100% at a deposition temperature of 260 °C for structures with an aspect ratio of 6.4 and a diameter of 0.2 μm.

Ruthenium films were grown on Si, SiO_2, TiO_2 and TiN substrates by the PMOCVD method from a mixture of Ru(EtCp)(dmpd) and oxygen.[25, 69] The limiting growth rate was 0.04 nm per cycle; however, the density of ruthenium in the film was lower while the specific resistance was much lower than those of bulk material. The results obtained are to some extent contradictory. On the one hand, no nucleation delay was observed.[69] On the other hand, the surfaces of the SiO_2 and TiN substrates were exposed to $TiCl_4$ vapours at ~400 °C in order to enhance nucleation of ruthenium.[25] Indeed, ruthenium films grown on the treated substrates were fine-grained, continuous and had a smoother surface. Improved properties of the Ru films were explained by the fact that treatment of the TiN surface (it is prone to adsorb atmospheric oxygen) with $TiCl_4$ vapours causes an increase in the surface concentration of Ti–O bonds that are more appropriate for nucleation of ruthenium. The degree of conformality of the coating was ~90% for structures with an aspect ratio of 17 and a diameter of 0.15 μm. It was found that this parameter is properly controlled by the flow rate (v) of the argon carrier gas used to transfer the precursor to the deposition chamber.

v /cm^3 min^{-1}	50	100	300	500
Degree of conformality (%)	100	80	35	0

A possible reason is high dilution of precursor vapours and, correspondingly, poorer conditions for diffusion into the interior of the structures during the pulses. Figure 14 presents the plots of the degree of conformality of the Ru films *vs*. deposition temperature for different precursors and deposition conditions.

Deposition of ruthenium on the surface of a low-dielectric-constant insulator (silica and hydrogen in the form of methyl groups) by PMOCVD from a mixture of Ru(EtCp)(dmpd) with oxygen at 250 °C was studied.[24] The concentration of methyl groups on the dielectric surface strongly affected the quality of the ruthenium film, namely, nucleation of ruthenium abruptly reduced with increasing concentration of methyl groups. UV irradiation or treatment of the dielectric surface with ozone prior to deposition led to a decrease in the content of methyl groups and to an increase in the concentration of OH groups that probably enhanced subsequent nucleation of ruthenium.

Two comparative studies of $Ru(dmpd)_2$ and Ru(EtCp)(dmpd) as precursors were reported.[70, 71] It was established that utilization of mixtures with oxygen requires control of the percentage of oxygen in order to preclude the formation of the oxide phase; the growth rates of ruthenium film per cycle were very low [several times lower than for the deposition from $Ru(EtCp)_2$ and Ru(EtCp)(dmpd)] and the specific resistance of the grown Ru films was rather high.

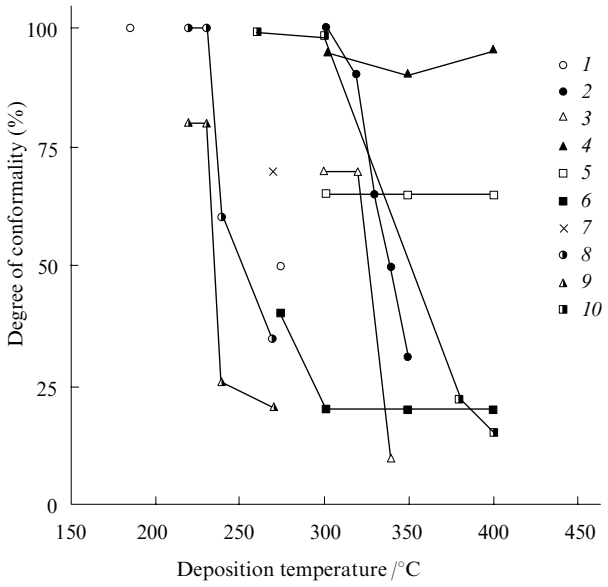


Figure 14. Degree of conformality of ruthenium coating plotted *vs*. deposition temperature for different precursors and deposition conditions [37] (*1*), 13 (*2*), 46 (*3*), 48 (*4–6*), 7 (*7*), 63 (*8*, *9*) and 68 (*10*).

4. Other ruthenium precursors

Ruthenium films were deposited from RuO_4 (yellow liquid with a boiling point of 130 °C and a vapour pressure of ~10 mm Hg at 25 °C) dissolved in an organic solvent whose properties are similar to those of the precursor (no details were reported) and hydrogen (1% mixture with nitrogen) as reducing agent.[72] Next,[73] researchers from the same group studied the possibility of deposition of conformal ruthenium films on 3D structures with an aspect ratio of 10 and a diameter of 0.01 μm by the MOCVD and PMOCVD methods. The degree of conformality of the films was more than 90%, the film density was ~12 g cm^{-3} and the specific resistance was ~20 μΩ cm. A toxicity study of RuO_4 revealed no indication of toxicity and confirmed that the oxide can be used in high-precision technologies. The mixture of the precursor and the solvent was called the total ruthenium solution (ToRuS). A clearly seen advantage of this precursor with the simplest chemical composition is that it contains no carbon–ruthenium bonds; it was also shown that carbon from the solvent is not a component of the coating. A novel organometallic precursor CHORUS™ developed at Air Liquide ALOHA and having no Ru–O bonds (vapour pressure is ~0.1 mm Hg at 23 °C) was proposed.[74] No chemical formula of the precursor and no details of the synthetic procedure are available. The authors [74] reported no nucleation delay when using this precursor and hydrogen as reagent gas. Ruthenium films (growth rate was 1.5 nm min^{-1} and the specific resistance

was 20 μΩ cm) grown on structures with an aspect ratio of 3 at 250 °C were characterized by a degree of conformality of 90%.

Ruthenium films were also deposited from various precursors based on carbonyls.[45,76] It was concluded[45] that the dimer $[Ru(Cp)(CO)_2]_2$ can be used in MOCVD processes with both flat-surface ($Ba_xSr_{1-x}TiO_3$) and 3D substrates (Si_3N_4). In the presence of oxygen, the deposition process accelerates and makes it possible to grow carbon-free ruthenium films. Pure ruthenium films grown at low deposition temperature (240 °C) on 3D structures with an aspect ratio of 3 and a diameter of 0.5 μm were characterized by good conformality and had a specific resistance of ~ 28 μΩ cm. Films grown at elevated temperature (> 350 °C) had a columnar structure on flat surfaces and were incontinuous inside 3D structures.

A nitrogen-containing precursor $Ru[Bu^tMe(amd)]_2(CO)_2$ having no Ru–O bonds was also used.[75] Deposition on complex-shape 3D structures with an aspect ratio of 40 and a diameter of 0.2 μm was carried out in both steady-state and pulsed regimes using ammonia as co-reactant. The degree of conformality of the coating was ~80%.

Deposition from cyclodiene-containing ruthenium precursors was studied.[76–78] Of two precursors, Ru(cod)(PhMe) and Ru(chd)(PhH), used for deposition of coatings in the temperature range 150–450 °C, the latter appeared to be more appropriate because the carbon impurity concentration in the films was lower.[76] Various schemes of thermal decomposition of precursor vapours were proposed.

A PMOCVD process was implemented using a precursor called IMBCHRu and oxygen as co-reactant.[77] The advantages of the precursor include the absence of nucleation delay for deposition on TiN surface (unlike the deposition on silica surface) and the absence of oxide phases at the interface with titanium nitride. A continuous ruthenium film coating of a 3D SiO_2 structure with an aspect ratio of 24 and a diameter of about 0.09 μm was characterized by a degree of conformality of nearly 100%; the specific resistance of the films was 36 μΩ cm. The IMBCHRu precursor was also used for deposition of ruthenium films by the PMOCVD method using plasma-activated ammonia in the temperature range 140–400 °C.[78] The process led to formation of dense Ru films (~11 g cm^{-3}) with no nucleation delay. By varying the plasma-activated ammonia pulse duration from 2 to 20 s the film density was increased from 9.5 to 11 g cm^{-3}.

Sari *et al.*[78] were the first who unambiguously stated practical implementation of the ALD process in the temperature range 250–400 °C. This is to some extent arguably from the standpoint of classical ideas of this regime because the conclusion was based only on the observation of a constant growth rate in the temperature range mentioned above. However, this observation can also be explained by the influence of other factors, *e.g.*, limitation of mass transfer or insufficient concentration of precursor vapours in the reaction zone.

V. Ruthenium dioxide films

Ruthenium dioxide films are usually prepared using the same precursors (mainly β-diketonates, ruthenocene and its derivatives in the presence of oxygen, as well as RuO_4) and apparatuses. Often, publications include the results of investigations of both ruthenium and its dioxide (ruthenia).[3,9,34,46,49,64,72,73] There are a few studies on the deposition and properties of ruthenium oxide *per se*.[107–117]

Among them, noteworthy is publication[116] concerning an interesting procedure for preparation of RuO_2 coatings used as catalysts. Namely, oxidation of metallic ruthenium particles in ozone stream to give RuO_4 was followed by elimination of oxygen and formation of RuO_2 on stainless steel substrate heated to 400 °C.

Taking the synthesis of oxide films as a whole, one can conclude that by varying the oxygen to precursor concentration ratio, the deposition method and reaction conditions, one can prepare films of specified composition, *viz.*, Ru, RuO_x or RuO_2. It should be noted that nucleation delays are not characteristic of ruthenium oxide films grown at high oxygen concentration. In some cases as, *e.g.*, in a study[114] on the possibility of using RuO_2 as lower electrode for MIM memory cells, RuO_2 was deposited on TiN surface pre-treated with argon, hydrogen or oxygen plasma to enhance nucleation of ruthenium.

Ruthenium dioxide forms polycrystalline films with the (100), (110), (002) and (101) grain orientations. The specific resistance of RuO_2 films depends strongly on the deposition conditions (usually, it is higher than ~50 μΩ cm) and increases as the oxygen to precursor concentration ratio increases.

Information on the conformality of RuO_2 coatings in 3D structures is scarce compared to corresponding data for ruthenium. However, one can conclude that trends of growth in this case are identical. Namely, the degree of conformality is nearly 80% at low deposition temperatures;[117] raising the temperature causes the degree of conformality to decrease and the structure of the deposited films to change (films with columnar structure are formed on the surface and incontinuous fine-grained coating are formed on lateral surfaces inside 3D structures).

VI. Examples of other ruthenium-containing materials

Not only ruthenium and its dioxide RuO_2, but also $SrRuO_3$ films grown on dielectric substrates SiO_2, Al_2O_3 and HfO_2 were studied as candidate materials for gate electrodes in metal–dielectric–semiconductor transistors.[118] Films were deposited at 500 °C in a cold-wall CVD reactor; other details were not reported. It was established that the electrophysical properties of ruthenium and $SrRuO_3$ are close, being better than the corresponding properties of RuO_2 (with respect to, *e.g.*, the leakage current through the dielectric gate). It is believed that both materials are promising for microelectronics applications.

The synthesis and properties of ruthenium films doped with platinum (up to 40 at.%) during the growth were reported.[119] The films were tested as electrodes for MIM memory cells in integrated circuits. Co-deposition from $Ru(Cp)(Pr^iCp)$ and $PtMe_3CpMe$ dissolved in tetrahydrofuran was carried out in the presence of oxygen. Doping led to significant improvement of the thermal stability of the ruthenium films, namely, reduction of their recrystallization

upon heat treatment and a decrease in the surface roughness of the coatings.

The possibility of growth of Ru–P amorphous films with a phosphorus content of ~15 at.% was studied.[120] This is a possible way to reduce (or exclude) copper diffusion along the Ru grain boundaries for multilayered copper metallization of integrated circuits. Deposition was carried out using *cis*-$RuH_2(PMe_3)_4$ as precursor in the temperature range 250–300 °C. The resultant films up to 30 nm thick became polycrystalline only upon additional thermal annealing at 500–700 °C.

VII. Conclusion

Growth of ruthenium-containing films by CVD methods has been intensively studied owing to practical interest in these films, first of all, application in high-precision technologies. At present, the main problem in the field is to grow thin, continuous, nanograined, dense and conductive ruthenium coatings with good adhesion to surfaces of small (< 100 nm) 3D structures with high aspect ratios. Yet another problem is nucleation of ruthenium on surfaces of different materials that are simultaneously used in microelectronics in, *e.g.*, MIM memory cells and integrated circuits.

Based on the available data, general regularities of formation of ruthenium-containing films are as follows.

The deposition rates can vary from a few fractions of a nanometre (for pulsed methods) to a few nanometres per second depending on the method (MOCVD, PMOCVD, PACVD), precursor type and process parameters. This is admissible for most applications in high-precision technologies. General drawbacks of most studies include fragmentary description of experimental conditions and results obtained, as well as the absence of detailed processing of kinetic data. In this connection, a relatively small number of publications containing description of models of processes under study and reaction schemes deserve particular attention. It is important that no proofs of the possibility of film growth in the ALD regime have been reported as yet.

Most authors report nucleation delays during film growth using different methods. It follows that surface processes contribute largely to nucleation and film growth. The maximum duration of the nucleation delay was found for MOCVD processes. It depends on the following factors:

— substrate material; nucleation phenomena are different for different types of substrates and lead to growth of incontinuous coarse-grained films with high surface roughness, low density, poor adhesive properties, low specific resistance; methods for control of nucleation on the surface taking into account the nucleation delay are available, namely, the use of two-step processes with pre-formed layer of uniformly distributed seeds at elevated temperature, UV irradiation or plasma treatment of the surface prior to deposition; abrupt enhancement of nucleation on all types of surfaces even at very low temperatures was attained using preliminarily deposited thin films of ruthenium nuclei or platinum group metals;

— deposition temperature; the deposition temperature seems to govern the growth processes; most authors reported observation of nucleation delays at reduced deposition temperatures; this undesired effect vanished as the deposition temperature increased;

— oxygen to precursor vapour concentration ratio in MOCVD processes; an increase in this ratio changes the coating composition from a metal to its oxide; as the partial pressure of oxygen in the mixture increases, oxygen diffusion in the near-surface region occurs, followed by the formation of oxide phases; this effect was not observed at low partial pressures of oxygen.

Many authors report the presence of carbon and, under particular conditions, oxygen impurities in the deposited ruthenium films. Both impurities lead to an increase, although to different extents, in the specific resistance of the ruthenium films. This is inadmissible for most practically important applications of these films in micro- and nanoelectronics.

Researchers pay little attention to the properties of deposited films and, in particular, to the specific resistance that belongs to the key parameters of he films. Different types of precursors demonstrate a decrease in the specific resistance as the film thickness and deposition temperature increase. This trend correlates with the increase in the proportion of continuous films and with the decrease in the carbon content in the films. This decrease was particularly pronounced in thermally annealed deposited films with high specific resistance. Other rarely studied properties include adhesion to surfaces of 3D structures (in some cases, it is insufficient) and the surface roughness of the coating. We believe these data are difficult to analyze because they are fragmentary; however, there is a clearly seen correlation with nucleation and growth of polycrystalline ruthenium films.

The most practically important issue is the deposition of thin continuous coatings on 3D structures (in most examples, these were trenches or cylindrical holes in dielectric materials with different aspect ratios). These data are scarce, were obtained for different structures and are therefore difficult to systematize. Also, a decrease in the degree of conformality with increasing deposition temperature seems to be of particular importance. In spite of a large scatter of data for same-type precursors, a trend towards dramatic decrease in the degree of conformality of the deposited coatings is clearly seen. Also, a decrease in the deposition temperature inside the 3D structures below particular values leads to poorer nucleation and to a decrease in the grain concentration gradient from the surface towards the interior of the film. Also, the degree of conformality of coatings decreases as the oxygen concentration in the reactions increases. We believe these data may be indicative of changes in mechanisms of deposition processes from surface-controlled (reaction is limited by surface processes) to vapour-phase limited ones. Problems with the delivery of precursor vapours to channels and small-diameter orifices in the 3D structures associated with minimization of integrated circuits should also be taken into account.

It seems appropriate to focus further research in the field of ruthenium-containing coatings on surface processes and, first of all, on problems in chemi- and physisorption of precursor vapours and on the chemical composition of intermediates of the decomposition reactions accompanying deposition of films.

References

1. D R Rolison, K Kuo, M Umana, D Brundage, R W Murray *J. Electrochem. Soc.* **126** 407 (1979)
2. R G Vadimsky, R P Frankenthal, D E Thompson *J. Electrochem. Soc.* **126** 2017 (1979)
3. M L Green, M E Gross, L E Papa, K J Schnoes, D Brasen *J. Electrochem. Soc.* **126** 2677 (1979)
4. M Nayak, S Ezhilvalavan, T Y Tseng, in *Handbook of Thin Film Materials* Vol. 3 (Ed. H S Nalwa) (San Diego, CA: Academic Press, 2001) p. 121
5. V Mistra, H Zhong, H Lazar *IEEE Electron Dev. Lett.* **23** 354 (2002)
6. I Goswami, R Laxman *Semicond. Int.* **27** 49 (2004)
7. O-H Kwon, J-H Kim, H-S Park, S-W Kang *J. Electrochem. Soc.* **151** G109 (2004)
8. W-H Kim, S-J Park, J-Y Son *Nanotechnology* **19** 45302 (2008)
9. W Chen, M Zhang, D W Zhang, S-J Ding, J-J Tan, M Xu, X-P Qu, L-K Wang *Appl. Surface Sci.* **253** 4045 (2007)
10. S Kim, T Karabacak, T-M Lu, N Koratkar *Proc. SPIE Conf.* **61720B** 85 (2006)
11. J Biener, T F Baumann, Y Wang, E J Nelson, S O Kucheyev, A V Hamza, M Kemell, M Ritala, M Leskelä *Nanotechnology* **18** 055303 (2007).
12. J A Augis, L L Hines *IEEE Trans. Comp. Hybrids Manufact. Technol.* **1** 46 (1978)
13. S-J Won, W-D Kim, C-Y Yoo, S-T Kim, Y-W Park, J-T Moon, M-Y Lee, in *The IEEE International Electron Devices Meeting (IEDM), Washington, DC, 2000* p. 789
14. K Sakiyama, S Onishi, K Ishihara, K Orita, T Kajiyama, N Hosoda, T Hara *J. Electrochem. Soc.* **140** 834 (1993)
15. H W Kim, B-S Ju, C-J Kang *Vacuum* **71** 481 (2008)
16. D Volger, P Doe *Solid State Technol.* **46** 35 (2003)
17. V Yu Vasil'ev *Russ. Microelectron.* **31** 224 (2002) [*Mikroelektronika* **31** 263 (2002)]
18. V Yu Vasilev, S M Repinskii *Russ. Chem. Rev.* **74** 452 (2005) [*Usp. Khim.* **74** 413 (2005)]
19. M Ritala, M Leskela, in *Handbook of Thin Film Materials* Vol. 3 (Ed. H S Nalwa) (San Diego, CA: Academic Press, 2001) p. 103
20. T Aaltonen, P Alen, M Ritala, M Leskela *Chem. Vap. Dep.* **9** 45 (2003)
21. O K Kwon, S H Kwon, H S Park, S W Kang *Electrochem. Solid State Lett.* **7** C46 (2004)
22. O K Kwon, S H Kwon, H S Park, S W Kang *J. Electrochem. Soc.* **151** C753 (2004)
23. J Lim, H Park, C Lee *Thin Solid Films* **475** 194 (2005)
24. J Heo, S Y Lee, D Eom, C S Hwang, H J Kim *Electrochem. Solid State Lett.* **11** G5 (2008)
25. B S Kim, S Y Kang, H S Seo, C S Hwang, H J Kim *Electrochem. Solid State Lett.* **10** D113 (2007)
26. V Yu Vasil'ev *Elektron. Tekhn., Ser. 2. Poluprovod. Pribory* 67 (2010)
27. D Barreca, A Buchberger, S Daolio, M Fabrizio *Langmuir* **15** 4537 (1999)
28. JP P. 11-035589 (1999)
29. US P. 7002033 (2006)
30. US P. 5962716 (1999)
31. S L Ingham, S W Magennis *J. Organomet. Chem.* **574** 302 (1999)
32. US P. 6576778 (2003)
33. US P. 6380080 (2002)
34. US P. 6844261 (2006)
35. T S Lazarz, Y Yang, N Kumar, D Y Kim, W Noh, G S Girolami, J R Abelson, in *Materials, Processes, Integration and Reliability in Advanced Interconnects for Mocro- and Nanoelectronics (Book Ser. Materials Research Society Symposium Proceedings) San Francisco, CA, 2007* Vol. 990, p. 103
36. V Yu Vasilyev, K P Mogilnikov, Y W Song *Electrochem. Solid State Lett.* **11** D89 (2008)
37. V Yu Vasilyev, K P Mogilnikov, Y W Song *J. Electrochem. Soc.* **155** D763 (2008)
38. V Yu Vasilyev, K P Mogilnikov, Y W Song *Cur. Appl. Phys.* **9** e148 (2009)
39. V Yu Vasilyev *Russ. Microelectron.* **39** 26 (2010) [*Mikroelektronika* **39** 28 (2010)]
40. V Yu Vasilyev *Russ. Microelectron.* **39** 199 (2010) [*Mikroelektronika* **39** 219 (2010)]
41. V Yu Vasilyev *Russian Microelectronics* **39** 262 (2010) [*Mikroelektronika* **39** 484 (2010)]
42. V Yu Vasilyev *Russ. Microelectron.* **40** 279 (2011) [*Mikroelektronika* **40** 300 (2011)]
43. V Yu Vasilyev *Russ. Microelectron.* **40** 403 (2011) [*Mikroelektronika* **40** 441 (2011)]
44. V Yu Vasilyev, S H Chung, Y W Song *Mikroelektronika* **42** 62 (2013)
45. K C Smith, Y-M Sun, N R Mettlach, R L Hance, J M White *Thin Solid Films* **376** 73 (2000)
46. C Manke, O Boissiere, U Weber, G Barbar, P K Baumann, J Lindner, M Tapajna, K Frolich *Microelectron. Eng.* **83** 2277 (2006)
47. I K Igumenov, P P Semyannikov, S V Trubin, N B Morozova, N V Gelfond, A V Mischenko, J Norman *Surf. Coat. Technol.* **201** 9003 (2007)
48. M Kadoshima, T Nabatame, M Hiratani, Y Nakamura, I Asano, T Suzuki *Jpn. J. Appl. Phys.* **41** l 347 (2002)
49. F Papadatos, S Skordas, Z Patel, S Consiglio, E Eisenbraun, in *Silicon Materials-Processing, Characterization and Reliability. (Book Ser. Materials Research Society Symposium Proceedings) San Francisco, CA, 2002* Vol. 716, p. 79
50. S K Dey, J Goswami, D Gu, H Waard, S Marcus, C Werkhoven *Appl. Phys. Lett.* **84** 1606 (2004)
51. T Aaltonen, M Ritala, K Arstila, J Keinonen, M Leskela *Chem. Vap. Dep.* **10** 215 (2004).
52. B C Hendrix, J J Welch, J F Roeder, Z Wang, C Xu, M Stawasz, T H Baum *ECS Transact.* **11** 569 (2007)
53. H Miura *Catal. Today* **28** 215 (1996)
54. T Aaltonen, A Rahtu, M Ritala, M Leskela *Electrochem. Solid State Lett.* **6** C130 (2003)
55. T Aaltonen, M Ritala, Y-L Tung, Y Chi, K Arstila, K Meinander, M Leskela *J. Mater. Res.* **19** 3353 (2004)
56. K J Park, D B Terry, S M Stewart, G N Parsons *Langmuir* **23** 6106 (2007)
57. S-J Park, W-H Kim, H-B-R Lee, W J Maeng, H Kim *Microelectron. Eng.* **85** 39 (2008)
58. S-J Park, W-H Kim, W J Maeng, Y S Yang, C G Park, H Kim, K-N Lee, S-W Jung, W K Seong *Thin Solid Films* **516** 7345 (2008)
59. S Y Kang, H J Lim, C S Hwang, H J Kim *J. Electrochem. Soc.* **149** C317 (2002)
60. S Y Kang, C S Hwang, H J Kim *J. Electrochem. Soc.* **152** C15 (2005)
61. S Y Kang, K H Choi, S K Lee, C S Hwang, H J Kim *J. Electroch. Soc.* **147** 1161 (2000)

62. Y Matsui, M Hiratani, T Nabatame, Y Shimamoto, S Kimura *Electrochem. Solid State Lett*. **4** C9 (2001)
63. Y Matsui, M Hiratani, T Nabatame, Y Shimamoto, S Kimura *Electrochem. Solid State Lett*. **5** C18 (2002)
64. F Papadatos, S Consiglio, S Skordas, E T Eisenbraun, A E Kaloyeros, J Peck, D Thompson, C Hoover *J. Mater. Res*. **19** 2947 (2004)
65. M Lisker, T Hur'yeva, E P Burte *ECS Trans*. **2** 55 (2007)
66. S-S Yim, D-J Lee, K-S Kim, M-S Lee, S-H Kim, K-B Kim *Electrochem. Solid State Lett*. **11** K89 (2008)
67. T Shibutami, K Kawano, N Oshima, S Yokoyama, H Funakubo *Electrochem. Solid State Lett*. **6** C117 (2003)
68. K Kawano, A Nagai, H Kosuge, T Shibutami, N Oshima, H Funakubo *Electrochem. Solid State Lett*. **9** C107 (2006)
69. S K Kim, S Y Lee, S W Lee, G W Hwang, C S Hwang, J W Lee, J Jeong *J. Electrochem. Soc*. **154** D95 (2007)
70. K Kawano, H Kosuge, N Oshima, H Funakubo *Electrochem. Solid State Lett*. **10** D60 (2007)
71. K Kawano, H Kosuge, N Oshima, H Funakubo *Electrochem. Solid State Lett*. **12** D80 (2009)
72. J Gatineau, R Yanagita, C Dussarrat *Microelectron. Eng*. **83** 2248 (2006)
73. J H Han, S W Lee, G J Choi, S Y Lee, C S Hwanga, C Dussarrat, J Gatineau *ECS Trans*. **19** 717 (2009)
74. J Gatineau, C Dussarrat *Surface Coat. Technol*. **201** 9146 (2007)
75. H Li, D B Farmer, R G Gordon, Y Lin, J Vlassak *J. Electrochem. Soc*. **154** D642 (2007)
76. A Schneider, N Popovska, I Jipa, U Zenneck *ECS Trans*. **2** 35 (2007)
77. T-K Eom, W Sari, K-J Choi, W-C Shin, J H Kim, D-J Lee, K-B Kim, H Sohn, S-H Kim *Electrochem. Solid State Lett*. **12** D85 (2009)
78. W Sari, T-K Eom, S-H Kim, H Kimb *J. Electrochem. Soc*. **158** D42 (2011)
79. V A Logvinenko *Termicheskii Analiz Koordinatsionnykh Soedinenii i Klatratov* (Thermal Analysis of Coordination Compounds and Clathrates) (Novosibirsk: Nauka, 1982)
80. I K Igumenov, Yu V Chumachenko, S V Zemskov, in *Problemy Khimii i Primeneniya β-Diketonatov Metallov* (The Problems of Chemistry and Application of Metal-β-Diketonates) (Moscow: Nauka, 1982)
81. A V Suvorov *Termodinamicheskaya Khimiya Paroobraznogo Sostoyaniya* (Thermodynamic Chemistry of Vapour State) (Leningrad: Khimiya, 1970)
82. P P Semyannikov, I K Igumenov, S V Trubin, I P Asanov *J. Phys. IV* **11** Pr3-995 (2001)
83. A A Bessonov, N B Morozova, N V Gelfond, P P Semyannikov, I A Baidina, S V Trubin, Yu V Shevtsov, I K Igumenov *J. Organomet. Chem*. **693** 2572 (2008)
84. A F Bykov, N B Morozova, I K Igumenov, S V Sysoev *J. Therm. Anal*. **46** 1551 (1996)
85. G Gervasio, R Bianchi, D Marabello *Chem. Phys. Lett*. **407** 18 (2005)
86. V G Syrkin *CVD-Metod. Khimicheskoe Parofaznoe Osazhdenie* (CVD-Method. Chemical Vapour Deposition) (Moscow: Nauka, 2000)
87. N B Morozova, Doctoral Thesis in Chemical Sciences, Institute of Inorganic Chemistry, Siberian Branch of the Russian Academy of Sciences, Novosibirsk, 2009
88. P R Raitby, J Lewis, C A Morewood, M C De Arellano, G P Shields *J. Clust. Sci*. **17** 13 (2006)
89. T S Knowles, M E Howells, B J Howlin, G W Smith, C A Amodio *Polyhedron* **13** 2197 (1994)
90. R Grobelny, B Jezowska-Trzebiatowska, W Wojciechowski *J. Inorg. Nucl. Chem*. **28** 2715 (1966)
91. J Johnson, A Johnson, G W Everett *J. Am. Chem. Soc*. **94** 1419 (1972)
92. J G Gordon, M J O'Connor, R H Holm *Inorg. Chim. Acta*. **5** 381 (1971)
93. G W Everett, J Johnson, A Johnson *J. Am. Chem. Soc*. **94** 6397 (1972)
94. K V Zherikova, N B Morozova, N V Kuratieva, T N Cheremisina *J. Struct. Chem*. **51** 589 (2010) [*Zh. Strukt. Khim*. **51** 605 (2010)]
95. M Lachdaf, T Hatanpaa, M Tiitta *J. Therm. Anal. Cal*. **64** 1171 (2001)
96. M A B Ribeiro da Silva, E Giera, M J S Monte *J. Alloys Compd*. **197** 105 (1993)
97. M A V Ribeiro da Silva, M J S Monte, E Gierab *J. Chem. Thermodyn*. **33** 369 (2001)
98. N B Morozova, K V Zherikova, P P Semyannikov, S V Trubin, I K Igumenov *J Therm. Anal. Cal*. **98** 395 (2009)
99. T Hashimoto, S Hara, Y Shiraishi, M Yamauchi *Inorg. Chim. Acta* **358** 2207 (2005)
100. *Metody Elementoorganicheskoi Khimii. Tipy Organicheskikh Soedinenii Perekhodnykh Metallov* (Methods of Organoelement Chemistry. Types of Organic Compounds of Transition Metals) Vol. 2 (Eds A N Nesmeyanov, K A Koshechkov) (Moscow: Nauka, 1975)
101. M O Albers, D C Liles, D G Robinson, A Shaver *Organometalics* **5** 2321 (1986).
102. A O Borissova, M Yu Antipin, D S Perekalin, K A Lyssenko *Cryst. Eng. Commun*. **10** 827 (2008)
103. WO 2004/041832 (2004)
104. P G Gassman, C H Winter *J. Am. Chem. Soc*. **110** 6130 (1988)
105. P Pertici, G Vitulli *J. Chem. Soc., Dalton Trans*. 1961 (1980)
106. Y-H Lai, T Y Chou, Y-H Song, C-S Liu *Chem. Mater*. **15** 2454 (2003)
107. I F Golovnev, E I Golovneva, V M Fomin, B M Kuchumov, I K Igumenov *Dokl. Phys*. **58** 1 (2013) [*Dokl. Akad. Nauk, Fiz*. **58** 1 (2013)]
108. J Vetrone, C M Foster, G-R Bai, A Wang, J Patel, X Wu *J. Mater. Res*. **13** 2281 (1998)
109. J M Lee, J C Shin, C S Hwang, H J Kim, C-G Suk *J. Vac. Sci. Technol. A* **16** 2768 (1998)
110. J-H Lee, J-Y Kim, S-W Rhee *Electrochem. Solid State Lett*. **2** 622 (1999)
111. S-E Park, H-M Kim, K-B Kim, S-H Min *J. Electrochem. Soc*. **147** 203 (2000)
112. P G Ganesan, M Eizenberg, C Dornfest *J. Electrochem. Soc*. **149** G510 (2002).
113. P G Ganesan, M Eizenberg *Mater. Sci. Eng*. **B103** 213 (2003)
114. T Eom, H W Kim, C Lee *J. Korean. Phys. Soc*. **44** 1083 (2004)
115. K E Swider-Lyons, C T Love, D R Rolison *J. Electrochem. Soc*. **152** C158 (2005)
116. R Hashaikeh, I S Butler, J A Kozinski *Thin Solid Films* **515** 1918 (2006)
117. K Kawano, H Kosuge, N Oshima, H Funakubo *Electrochem. Solid State Lett*. **9** C175 (2006)
118. M Tapajna, P Pesecny, R Lupta, K Husekova, K Frohlich, L Harmatha, J C Hooker, F Roozeboomd, J Jergel *Mater. Sci. Semicond. Proc*. **7** 271 (2004)

119. S Y Kang, S Y No, J-H Choi, C S Hwang, H J Kim *Electrochem. Solid State Lett.* **8** C12 (2005)
120. J Shin, A Waheed, W A Winkenwerder, H-W Kim, K Agapiou, R A Jones, G S Hwang, J G Ekerdt *Thin Solid Films* **515** 5298 (2007)